Geochronologies from the Kathmandu Valley UNESCO World Heritage Site: Optically Stimulated Luminescence measurement of monument foundation sediments and radiocarbon measurement of timbers.

Kinnaird, T.C.[1,] and Simpson, I.A.[2]

[1]*School of Earth and Environmental Sciences, University of St Andrews*
[2]*School of Biological and Environmental Sciences, University of Stirling*

Nepal was struck by two major earthquakes on the 25th April and the 12th May 2015, which devastated large areas of the county, with substantial loss of life and livelihoods, and destroying both rural and urban infrastructure and property. The earthquakes and associated aftershocks damaged and destroyed much of Nepal's unique cultural heritage, including monuments within the Kathmandu Valley's UNESCO World Heritage Site of Universal Outstanding Value. These damaged monuments are currently subject to a major program of consultation, reconstruction and conservation. As part of this, geoarchaeological investigations are underway on the foundation sediments of the collapsed monuments within the damaged Durbar Squares of Hanuman Dhoka and Bhaktapur and the temple complex of Pashupati. This report summaries: a) the OSL investigations on foundation sediments to the Changu Narayan and Vatsala Temples (Bhaktapur) and Jaisideval, Kathamandap, Pashupati and Trailokya Mohan Temples (Kathmandu; Table 1).; b) the radiocarbon measurements from timbers salvanged from the Kasthsmandap monument

The background to these investigations, and the descriptions of the methods and protocols used in determining luminescence ages have been presented in three interim reports – Kinnaird et al. (2016), Kinnaird and Simpson (2018) and Kinnaird et al. (2018). The technical details are not re-produced here, but a summary of the techniques and protocols employed in the OSL analyses is appended in 'Supplementary Data Files'. All data tables are re-produced.

OSL dates from the monument foundation sequences (Table 2) fall into several populations: 1.) those that represent the natural sand and silt based accumulations beneath the urban sediments (Jaisideval, Pashupati, Kasthamandap and Changu Narayan); 2.) those that document the earliest phase of human activity in the area, synchronous with agriculture and woodland clearance, from the 10th-9th centuries BC (Kasthamandap and Vatsala); 3.) those that relate to early urban activity in the areas in the first centuries BC and AD (Kasthamandap and Vatsala), suggesting that urbanisation may have been contemporaneous between the city sites of Kathmandu and Bhaktapur; and 4.) those that relate to construction and modification of the monuments (Jaisideval, Kathamandap, Pashupati, Trailokya Mohan, Changu Narayan and Vatsala). The sediment ages suggest the following preliminary chronology for construction of the monuments:

- 1st phase construction at Kasthamandap and Changu Narayan Temple (7th- 8th century AD); potentially a century earlier at Pashupati Temple (6th century AD);
- 2nd phase construction at Kasthamandap and Changu Narayan Temple (8th century AD);
- 1st phase construction of Jaisideval Temple and Trailokya Mohan Temple (10th-11th centuries AD);
- 1st phase construction of Nine Storey Temple (13th-14th century AD);
- later modifications at Nine Storey Temple and Jaisideval Temple from the 14th century AD through to the late 16th century AD

The emerging sediment chronologies are demonstrating a long history of human activity associated with these temple sites, from the onset of urbanisation in the first centuries BC / AD to early monument construction from the 7th century AD. When coupled with geoarchaeological investigations on the soils and sediments forming the foundations to these monuments, new narratives on the site formation processes and early monument construction are being developed, that contribute to our knowledge and appreciation of these damaged sites.

Radiocarbon measurements offers complementary insight to the OSL chronology of the Kasthamandap monument through the dating of the four main construction timbers (Table 3). One of these timbers (C1) has an early date of 688 (22.8%) 753calAD, 758 (72.6%) 890cal AD at 95.4% probability, corresponding almost precisely to the later Licchavi period OSL foundation dates. The three other construction timbers (C2, C3 and C4) are later and in their ages from ca. 1018AD – 1220 AD, with C4 a slightly younger timber. These three dates are of particular significance as they suggest significant construction at the site during the later transitional kingdom period for which there is a current paucity of archaeological evidence. They also suggest that there had been a later remodelling of the monument superimposed on the Licchavi period foundations with one of the timber (C1) incorporated into the remodelling. Two dates were obtained from the repaired C3 timber; the dates of the main timber and the repair are virtually identical suggesting that the repair was undertaken from the same original timber and at the time of the damage. The earliest radiocarbon date in the set is from the bracket (Br1) (424 (95.4%) 565calAD) and further confirms the Licchavi period origins of the monument.

References

Kinnaird, T.C., Simpson, I.A. and Sanderson, D.C.W. 2016. OSL dating of sediments revealed during rescue excavations at Hanuman Dhoka and Bhaktapur Durbar Square, Kathmandu, Nepal. *SUERC OSL dating report*. SUERC, University of Glasgow

Kinnaird, T.C. and Simpson, I.A. 2017. Kathmandu Valley OSL Measurements Series: Nine Storey Palace Foundations. *CERSA Luminescence Interim Report.* School of Earth and Environmental Sciences, University of St Andrews

Kinnaird, T.C., Simpson, I.A. and Bradley, S. 2018. Kathmandu Valley OSL Measurements Series: Changu Narayan, Jaisideval, Pashupati and Trailokya Mohan. *CERSA Luminescence Interim Report.* School of Earth and Environmental Sciences, University of St Andrews

Year	Field Profile ID	CERSA lab code	Context	Description	Archaeological significance?
	Changu Narayan Temple, Bhaktapur [27.716274°, 85.427891°]				
2018	CGN17-1	229	[6024]	89 cm depth; 10YR 5/4, Sandy Silt loam	Base stratigraphic context of foundation deposits, below first wall and above natural sediments.
	CGN17-2	230	[6017]	61 cm depth; 10YR 4/4, Sandy clay loam	Stratigraphic context immediately beneath second wall in foundation stratigraphy.
	CGN17-3	231	[6011]	37 cm depth; 10YR 3/3, Silty loam.	Stratigraphic context immediately beneath third wall in foundation stratigraphy; below surface platform.
	Vatsala Temple, Bhaktapur [27.671941°, 85.428418°]				
2016	OSL1	*2859	[667]		constrain onset of human activity (in this area of Kathmandu valley)
	OSL2	*2860	[668]		constrain onset of urban human activity
	Jaisideval Temple, Kathmandu [27.700238°, 85.304251°]				
2018	JSF17-1 Tr3	232	[2354]	220 cm depth; 10YR 4/2; Loamy sand	Stratigraphic context beneath last layer of brick at base of stratigraphy (east facing)
	JSF17-2 Tr3	233	[2351]	220 cm depth; 5Y 3/1; Sandy silt loam	Stratigraphic context beneath last layer of brick at base of stratigraphy (south facing)
	JSF17-3 Tr3	234	[2334]	68 cm depth; 10YR 6/3; sand	Stratigraphic context sand horizon and below upper brick deposits
2016	JSD16 AT5/6	74	[2196]		beneath third plinth (from outer side) of monument; cultural surface preceding monument.
	JSD16 AT3 -1	75	[2231]	420 cm beneath surface of post-earthquake monument; culturally deposited sand horizons	beneath second plinth (from outer side) of monument; cultural surface preceding monument.
	JSD16 AT3 -2	76	[2198]		
	Kasthamandap Temple, Hanuman Dhoka Durbar Square, Kathmandu [27.703931°, 85.305888°]				
2017	Kasthamandap, HMD16, M5 [1286]	77	[1298]	2.60m below surface of post- earthquake monument; beneath M5 trench cross-wall	foundation soil; TPQ for construction of Kasthamandap monument.
2016	OSL Env 2	*2851	[422]	190 cm depth;	constrain onset of human activity (in this area of Kathmandu valley)
	OSL Env 4	*2852	[339]	140 cm depth;	constrain onset of urban

					human activity
	OSL1	[*]2853	[491]	40 cm depth;	
	OSL2	[*]2854	[321]	135 cm depth;	
	OSL3	[*]2855	[346]	170 cm depth;	TPQ for construction of
	OSL4	[*]2856	[419-345]	210 cm depth;	wall
	OSL5	[*]2857	[419-354]	210 cm depth;	
	OSL6	[*]2858	[404=406]	195 cm depth;	

Nine Storey Palace Temple, Hanuman Dhoka Durbar Square, Kathmandu [27.704070°, 85.307720°]

2018	MDT Tr3 [4]	132	[4]	-	Early environment with cultural inclusions
	MDT Tr3 [10,c]	133	[10,cut]	258 cm depth;	Beneath cross-wall; earliest 'urban' sediments
	MDT Tr3 [10,b]	134	[10,base]	258 cm depth;	Base of context 10; earliest 'urban' sediments
	MDT Tr3 [16B]	135	[16B, sand]	-	Early environment between sediments with cultural inclusions.
	MDT Tr3 [19]	136	[19]	90 cm depth;	Beneath later lower wall

Pashupati Temple, Kathmandu [27.710620°, 85.348581°]

2018	PASH17-1 Tr5	235	[508]	238 cm depth; 2.5Y 5/3; medium loamy sand	Initial foundation sediment context, found across the trench
	PASH17-2 Tr5	236	[510A]	250 cm depth; 2.5Y 4/3; medium loamy sand	Sediment context beneath wall remains; constructed before temple foundations.

Trailokya Mohan Temple, Hanuman Dhoka Durbar Square [27.703955°, 85.306298°]

2018	TLM17-1	237	[5162]	340 cm depth; 5YR 3/2; silty clay	Foundation wall base sediment

Table 1: OSL Sample details

Year	Lab code	Field ID	Age / ka	Age / Calendar years
Changu Narayan Temple, Bhaktapur				
2018	CERSA229	CGN17-1	3.08 ± 0.09	1060 ± 210 BC
	CERSA230	CGN17-2	1.39 ± 0.02	AD 630 ± 90
	CERSA231	CGN17-3	1.27 ± 0.02	AD 750 ± 90
Vatsala *Temple, Bhaktapur*				
'16	SUTL2859	Vatsala OSL1	2.79 ± 0.10	770 ± 100 BC
	SUTL2860	Vatsala OSL2	2.10 ± 0.08	80 ± 80 BC
Jaisideval Temple, Kathmandu				
2018	CERSA232	JSF17-1 Tr3	0.54 ± 0.01	AD 1480 ± 70
	CERSA233	JSF17-2 Tr3	4.14 ± 0.05	2120 ± 200 BC
	CERSA234	JSF17-3 Tr3	0.65 ± 0.01	AD 1340 ± 200
2017	CERSA074	JSD16, AT5/6 [2196]	0.50 ±0.06	AD1520 ± 60
	CERSA075	JSD16, AT3 [2231]	0.96 ±0.06	AD1060 ± 60
	CERSA076	JSD16, AT3 [2198]	1.12 ±0.08	AD900 ± 80
Jaisideval Temple, Kathmandu				
'17	CERSA077	HMD16, M5 [1286]	1.92 ±0.09	AD100 ± 90
2016	SUTL2851	Kas OSL Env 2	3.07 ± 0.14	1050 ± 140 BC
	SUTL2852	Kas OSL Env 4	1.91 ± 0.09	AD 100 ± 150
	SUTL2853	Kas OSL1	2.11 ± 0.02	100 ± 80 BC
	SUTL2854	Kas OSL2	1.39 ± 0.16	AD 630 ± 160
	SUTL2855	Kas OSL3	1.55 ± 0.14	AD 470 ± 140
	SUTL2856	Kas OSL4	1.35 ± 0.08	AD 660 ± 200
	SUTL2857	Kas OSL5	2.10 ± 0.07	80 ± 70 BC
	SUTL2858	Kas OSL6	1.27 ± 0.05	AD 750 ± 60
Nine Storey Palace Temple, Kathmandu				
2017	CERSA133	NDT Tr3 [10, cut]	0.58 ± 0.07	AD 1440 ± 70
	CERSA134	NDT Tr3 [10, base]	0.68 ± 0.04	AD 1330 ± 40
	CERSA136	MDT Tr3 [19]	0.43 ± 0.07	AD 1590 ± 70
Pashupati Temple, Kathmandu				
'18	CERSA235	PASH17-1 Tr5	1.50 ± 0.02	AD 520 ± 120
	CERSA236	PASH17-2 Tr5	3.72 ± 0.04	1700 ± 190 BC
Trailokya Mohan Temple, Kathmandu				
'18	CERSA237	TLM17-1	0.98 ± 0.02	AD 1040 ± 120

Table 2: Quartz OSL SAR sediment ages (Kinnaird et al., 2016; 2018; Kinnaird and Simpson, 2017)

Field code	Laboratory code	Radiocarbon Age BP	Calibrated age ranges BC/AD
HMD16 C1 (Pillar)	SUERC-78833 (GU47143)	1219 ± 35	68.2% probability 725 (7.5%) 738calAD 768 (7.4%) 780cal AD 788 (53.3%) 875calAD 95.4% probability **688 (22.8%) 753calAD** **758 (72.6%) 890cal AD**
HMD16 C1 (Pillar - outer)	SUERC-81870 (GU48919)	1135 ± 28	68.2% probability 885 (68.2%) 969calAD 95.4% probability **777 (3.8%) 791calAD** **805 (6.6%) 843cal AD** **860 (85.0%) 985cal AD**
HMD16 C2 (Pillar)	SUERC-78834 (GU47144)	898 ± 35	68.2% probability 1046 (31.2%) 1093calAD 1121 (11.4%) 1140cal AD 1147 (25.6%) 1189calAD 95.4% probability **1038 (95.4%) 1214calAD**
HMD16 C3 (Pillar)	SUERC-74764	943± 28	68.2% probability 1034 (14.1%) 1050calAD 1083 (40.0%) 1127cal AD 1135 (14.1%) 1151calAD 95.4% probability **1027 (95.4%) 1156calAD**
HMD16 C3 (Pillar - outer)	SUERC-81871 (GU48920)	901 ± 28	68.2% probability 1046 (34.5%) 1093calAD 1121 (12.2%) 1140cal AD 1147 (21.6%) 1183calAD 95.4% probability 1039 (95.4%) 1209calAD
HMD16 C3 (Pillar 'tendon repair')	SUERC-74763	967± 29	68.2% probability 1022 (27.4%) 1048calAD 1088 (32.4%) 1123cal AD 1139 (8.5%) 1149calAD 95.4% probability **1018 (95.4%) 1155calAD**
HMD16 C4 (Pillar)	SUERC-78835 (GU47145)	885 ± 35	68.2% probability 1051 (20.4%) 1083calAD 1127 (4.1%) 1135cal AD 1151 (43.7%) 1212calAD 95.4% probability **1039 (95.4%) 1220calAD**
HMD16 B1 (Cross Beam)	SUERC-81869 (GU48918)	952 ± 28	68.2% probability 1028 (19.0%) 1050calAD 1084 (37.0%) 1125cal AD 1136 (12.2%) 1151calAD 95.4% probability **1024 (95.4%) 1155calAD**
HMD16 Br1 (Bracket)	SUERC-74765	1554 ± 28	68.2% probability 430 (51.6%) 493calAD 511 (3.8%) 517cal AD 529 (12.7%) 545calAD 95.4% probability **424 (95.4%) 565calAD**

Table 2: Radiocarbon measurements. Kasthamandap timbers, Kathmandu Valley

Supplementary Data Files

The following sections provide the technical background to the OSL investigations of the sediment samples from the foundations to the Changu Narayan and Vatsala temples, Bhaktapur and Jaisideval, Kathamandap, Pashupati and Trailokya Mohan Temples, Kathmandu.

Sample preparation and analysis of the samples collected in 2015 (Kathamandap Temple, Kathmandu and Vatsala Temple, Bhaktapur) were undertaken in the luminescence laboratories at the Scottish Universities Environmental Research Centre (SUERC). Sample preparation and analysis of the 2016-2017 sample sets (2016 -Jaisideval & Kathamandap Temples, Kathmandu; 2017-Jaisideval, Pashupati & Trailokya Mohan temples, Kathmandu and Changu Narayan Temple, Bhaktapur) were undertaken in the luminescence laboratories within the School of Earth and Environmental Sciences at the University of St Andrews. With the latter, dose rate determinations were undertaken at the Environmental Radioactivity Laboratory at the University of Stirling.

Sample preparation

Mineral preparation followed a standardised protocol: all samples were wet sieved at 90 and 250 µm, then the 90-250 µm treated in 1M Hydrochloric acid (HCl) for 10 minutes, 40% Hydrofluoric acid HF for 40 minutes and 1M HCl for 10 minutes. The acid etched, 90- 250 µm mineral fractions were then density separated in heavy liquids solutions of 2.51, 2.58, 2.64 and 2.74 gcm^{-3}, providing concentrates of K feldspar (2.51-2.58 gcm^{-3}), plagioclase (2.58-2.64 gcm^{-3}), quartz (2.64-2.74 gcm^{-3}) and the heavy minerals (>2.74 gcm^{-3}). The 90-250 µ, HF-etched, 2.64-2.74 gcm^{-3} fractions were re-sieved at 150 µm, then either the 90-150 µm or 150-250 µm fraction dispensed to disc for equivalent dose determinations.

Equivalent dose determinations

All OSL measurements were carried out using Risø TL-OSL DA-20 automated dating systems. The technical specifications of the instruments at SUERC and St Andrews are provided in Kinnaird et al. (2016) and Kinnaird and Simpson (2017).

Equivalent dose (De) determinations were determined by OSL on 16-58 aliquots per sample using a single aliquot regeneration dose (SAR) OSL protocol (cf. Murray and Wintle, 2000; Kinnaird et al., 2017). This was implemented using regenerative doses of *(1)*, 2.5, 5, 10 and 30 Gy, with additional cycles for zero dose (0 Gy), repeat or 're-cycling' dose (*(1)*, 2.5 Gy) and IRSL contamination (*(1)*, 2.5 Gy). A test dose of 1 Gy was used throughout. An additional regenerative dose of 1 Gy was included in the SAR OSL protocols at SUERC (in *italicised* numbers above).

Dose response curves were fitted with an exponential function, with the growth curve fitted through the zero and the repeat dose recycling points. Aliquots were rejected from further analysis if they failed sensitivity checks (based on test dose response), SAR acceptance criteria checks, or had significant IRSL response coupled with anomalous luminescence behaviour (Table S1). Further details are provided in the respective dating reports.

De distributions were appraised for homogeneity using graphical plotting (Kernel Density Estimate Plots and Abanico Plots; Dietze et al., 2013) and statistical aids (dose models specific to luminescence dating in the R package *Luminescence*). Different permutations of the assimilation of

De to obtain the burial dose were considered including weighted combinations and statistical dose models (i.e. Guérin et al., 2017). The weighted mean of the De distribution was used in calculation of the luminescence age.

Dose rate determinations

Dose rate estimates to these sediments were assessed using a combination of field gamma spectrometry (FGS), high-resolution gamma spectrometery (HRGS), thick source beta counting (TSBC) and inductively coupled plasma mass spectrometry (ICP-MS), reconciled with each other and with the water contents and micro-dosimetry of the model. HRGS and TSBC were used at SUERC, whereas, a combination of HRGS and ICP-MS was used at St Andrews.

Field (ranging from 2 to 20% of dry weight) and saturated (20 to 27% of dry weight) water contents were determined for all samples in the laboratory, with working values of 9 to 20 % adopted for effective dose rate evaluation. Activity concentrations of potassium, uranium and thorium as obtained from HRGS and ICPMS were converted into dry infinite matrix dose rates (Table S2). This data, corrected for water content, were combined using weighted statistics with the measured beta (SUERC) and gamma (SUERC and St Andrews) dose rates, and an estimate of the cosmic dose contribution (Prescott and Hutton, 1994), to obtain total environmental dose rates (Table S3). Further details are provided in the respective dating reports.

Age determinations

OSL SAR dating utilises extracted quartz from the samples to determine the radiation dose experienced by the sediments since their last zeroing event assumed to be by exposure to light prior to final deposition, the burial dose, Db. To obtain a depositional age, it is necessary to reduce each De distribution to a single Db. The interim reports present the De distributions as Kernel Density Estimate Plots and Abanico Plots; here (appendix A), apparent ages were estimated for each aliquot (with the dose rate specific to that grain size fraction) and these are presented in Appendix A as the aforementioned plots.

Age estimates were determined by dividing the burial dose (Gy) by the environmental dose rate (mGy a^{-1}).

References

Dietze, M., Kreutzer, S., Fuchs, M. C., Burow, C., Fischer, M., and Schmidt, C. 2013, A practical guide to the R package Luminescence. *Ancient TL*, **32**, p. 11-18.

Guérin, G., Mercier, N. and Adamiec, G. 2011, Dose-rate conversion factors: update. *Ancient TL*, **29**, p. 5-8.

Kinnaird, T. C., Dawson, T., Sanderson, D. C. W., Hamilton, D., Cresswell, A. and Rennel, R. 2017. Chronostratigraphy of an eroding complex Atlantic round house, Baile Sear, Scotland. *Journal of Coastal and Island Archaeology*, v. in press.

Kinnaird, T.C. and Simpson, I.A. 2016. OSL dating of sediments revealed during rescue excavations at Hanuman Dhoka and Bhaktapur Durbar Square, Kathmandu, Nepal. *Technical Report*, SUERC, Glasgow

Kinnaird, T.C. and Simpson, I.A. 2017. Kathmandu Valley and Nepalese Terai OSL Measurements Series: Dohani, Jaisideval, Kasthamandap. *Technical Report*, University of St Andrews, St Andrews.

Murray, A. S. and Wintle, A. G. 2000. Luminescence dating of quartz using an improved single-aliquot regenerative-dose protocol. *Radiation Measurements*, **32**, p. 57-73.

Prescott, J. R. and Hutton, J. T. 1994. Cosmic ray contributions to dose rates for luminescence and ESR dating: Large depths and long-term time variations. *Radiation Measurements*, **23**, p. 497-500.

Year	Lab code	Sensitivity / counts Gy^{-1}	Recuperation /% [h, i]	Recycling ratio	IRSL response /%	Dose recovery
		Changu Narayan Temple, Bhaktapur				
2018	229	1990 ± 360	0.3 ± 0.5[h]	0.99 ± 0.06	0.3 ± 0.7	1.03 ± 0.05
	230	1670 ± 260	1.3 ± 0.5[h]	1.00 ± 0.06	1.1 ± 2.1	1.04 ± 0.04
	231	2230 ± 380	2.9 ± 1.1[h]	1.05 ± 0.04	0 ± 0.2	1.00 ± 0.05
		Vatsala Temple, Bhaktapur				
'16	*2859	2914 ± 1942	0.02 ± 0.05[i]	1.01 ± 0.06	0.7 ± 1.1	1.07 ± 0.06
	*2860	2302 ± 1032	-0.02 ± 0.04[i]	0.99 ± 0.06	-0.2 ± 1.6	1.05 ± 0.06
		Jaisideval Temple, Kathmandu				
2018	232	2960 ± 1320	11.2 ± 11.7[h]	0.96 ± 0.09	16.8 ± 18.6	1.01 ± 0.05
	233	153890 ± 263640	3.5 ± 6.2[h]	0.99 ± 0.04	47.4 ± 19.1	1.00 ± 0.12
	234	101500 ± 73380	6.2 ± 3.2[h]	0.96 ± 0.07	61.3 ± 10.7	1.09 ± 0.08
2017	74	780 ± 150	1.5 ± 2.8[h]	0.98 ± 0.04	1.81 ± 5.25	1.06 ± 0.04
	75	1560 ± 2070	3.8 ± 4.1[h]	0.99 ± 0.10	4.75 ± 9.05	1.04 ± 0.11
	76	63750 ± 38620	1.5 ± 0.3[h]	1.01 ± 0.04	83.1 ± 2.7	0.99 ± 0.04
		Kasthamandap Temple, Kathmandu				
'17	77	47280 ± 23220	1.0 ± 0.2[h]	0.99 ± 0.02	87.1 ± 7.1	1.00 ± 0.01
2016	*2851	6329 ± 8310	0.07 ± 0.09[i]	1.08 ± 0.05	8.4 ± 4.2	1.01 ± 0.06
	*2852	58139 ± 29701	0.02 ± 0.01[i]	1.01 ± 0.01	25.2 ± 2.6	0.94 ± 0.05
	*2853	7961 ± 5315	0.01 ± 0.01[i]	1.01 ± 0.01	0.2 ± 0.3	0.97 ± 0.05
	*2854	2554 ± 5227	0.04 ± 0.03[i]	0.97 ± 0.02	9.1 ± 6.9	1.00 ± 0.06
	*2855	3660 ± 5752	0.04 ± 0.03[i]	0.98 ± 0.01	9.9 ± 5	1.06 ± 0.06
	*2856	1071 ± 877	0.01 ± 0.05[i]	1.04 ± 0.05	5.8 ± 2.5	0.98 ± 0.06
	*2857	26683 ± 16172	0.02 ± 0.01[i]	1.04 ± 0.03	19.3 ± 4.7	0.92 ± 0.05
	*2858	1323 ± 1303	0.04 ± 0.08[i]	1.04 ± 0.05	2.9 ± 3.4	1.02 ± 0.06
		Nine Storey Palace Temple, Kathmandu				
2017	133	47960 ± 28930	4.8 ± 0.9[h]	1.03 ± 0.03	42.7 ± 9.7	1.00 ± 0.04
	134	5280 ± 4960	6.1 ± 2.3[h]	1.01 ± 0.01	19.1 ± 11.6	0.98 ± 0.04
	136	5950 ± 2710	6.3 ± 1.9[h]	0.99 ± 0.01	13.8 ± 11.5	1.01 ± 0.05
		Pashupati Temple, Kathmandu				
'18	235	248740 ± 159190	3.3 ± 1.3[h]	1.01 ± 0.01	60.4 ± 4.0	0.98 ± 0.01
	236	1073470 ± 570100	1.9 ± 0.4[h]	1.00 ± 0.02	60.0 ± 4.5	0.99 ± 0.02
		Trailokya Mohan Temple, Kathmandu				
'18	237	2710 ± 1360	3.7 ± 2.5[h]	1.03 ± 0.04	30.4 ± 23.6	1.01 ± 0.04
2018	233*	2690 ± 740	4.4 ± 3[h]	0.99 ± 0.06	3.6 ± 3.6	1.04 ± 0.07
	234*	15800 ± 16200	11.5 ± 8.9[h]	1.01 ± 0.05	53.7 ± 15.2	1.00 ± 0.04
	235*	2730 ± 860	3.1 ± 2.1[h]	0.99 ± 0.04	10 ± 14.9	1.02 ± 0.05
	236*	276700 ± 180810	2.3 ± 1.2[h]	1.01 ± 0.05	69.2 ± 3.8	0.97 ± 0.06

*Table S1: SAR quality criteria, 200μm HF-etched quartz; [h] Lx/Tx of zero dose point as a percentage of the Lx/Tx of the natural signal; [i] zero dose in Gy; *repeats, following high IRSL responses; further HCl and HF acid washes lowered IRSL for CERSA233 and 236*

	Lab code	Radionuclide concentrations [a,b]			Dose rates, Dry [c] / mGy a⁻¹			Dose rates, Wet [d] / mGy a⁻¹
		K / %	U / ppm	Th / ppm	Alpha	Beta	Gamma	
				Changu Narayan Temple, Bhaktapur				
2018	229[a]	2.89 ± 0.24	4.73 ± 0.26	14.02 ± 0.78	23.6 ± 0.9	3.04 ± 0.2	1.92 ± 0.08	1.67 ± 0.11
	230[a]	2.91 ± 0.24	4.65 ± 0.24	12.08 ± 0.68	21.9 ± 0.9	3.01 ± 0.2	1.82 ± 0.07	1.66 ± 0.09
	231[a]	2.83 ± 0.24	4.82 ± 0.28	12.26 ± 0.71	22.5 ± 0.9	2.97 ± 0.2	1.83 ± 0.08	1.52 ± 0.11
				Vatsala Temple, Bhaktapur				
'16	*2859[a]	2.72 ± 0.08	3.46 ± 0.31	15.38 ± 0.71	21.0 ± 1.0	3.21 ± 0.08	1.84 ± 0.05	1.50 ± 0.13
	*2859ᵦ[a]	2.83 ± 0.05	4.55 ± 0.22	19.51 ± 0.27	27.1 ± 0.6	3.57 ± 0.05	2.21 ± 0.03	-
	*2860[a]	2.79 ± 0.11	4.60 ± 0.65	18.58 ± 1.50	26.5 ± 2.1	3.52 ± 0.14	2.16 ± 0.11	1.57 ± 0.14
	*2860ᵦ[a]	2.83 ± 0.05	4.55 ± 0.22	19.51 ± 0.27	27.1 ± 0.6	3.57 ± 0.05	2.21 ± 0.03	-
				Jaisideval Temple, Kathmandu				
2018	232[a]	3.29 ± 0.27	4.25 ± 0.23	9.43 ± 0.53	18.8 ± 0.8	3.17 ± 0.22	1.74 ± 0.08	1.74 ± 0.17
	233[a]	3.33 ± 0.27	6.88 ± 0.33	15.54 ± 0.83	30.7 ± 1.1	3.67 ± 0.22	2.34 ± 0.09	1.75 ± 0.15
	234[a]	3.37 ± 0.27	2.37 ± 0.14	5.31 ± 0.33	10.5 ± 0.5	2.91 ± 0.21	1.36 ± 0.07	1.23 ± 0.10
2017	74[b]	2.69 ± 0.08	4.66 ± 0.14	20.15 ± 0.6	27.7 ± 0.6	2.99 ± 0.07	2.14 ± 0.04	1.94 ± 0.10
	75[b]	3.93 ± 0.12	5.03 ± 0.15	22.06 ± 0.66	30.1 ± 0.6	3.99 ± 0.10	2.57 ± 0.05	1.95 ± 0.10
	75ᵦ[b]	3.93 ± 0.12	4.99 ± 0.15	22.22 ± 0.67	30.1 ± 0.6	3.98 ± 0.10	2.58 ± 0.05	-
	76[b]	3.77 ± 0.11	3.03 ± 0.09	11.54 ± 0.35	16.9 ± 0.4	3.39 ± 0.09	1.81 ± 0.03	1.91 ± 0.10
				Kasthamandap Temple, Kathmandu				
'17	77[b]	3.16 ± 0.09	8.15 ± 0.24	32.34 ± 0.97	46.3 ± 1	4.03 ± 0.09	3.23 ± 0.06	2.52 ± 0.13
2016	*2851[a]	3.18 ± 0.05	4.83 ± 0.23	19.30 ± 0.26	27.7 ± 0.7	3.89 ± 0.06	2.31 ± 0.03	2.12 ± 0.19
	*2852[a]	3.89 ± 0.08	4.87 ± 0.35	22.02 ± 0.56	29.8 ± 1.1	4.57 ± 0.08	2.63 ± 0.05	1.92 ± 0.17
	*2852ᵦ[a]	3.59 ± 0.06	5.71 ± 0.30	23.43 ± 0.32	33.2 ± 0.9	4.49 ± 0.07	2.73 ± 0.04	-
	*2853[a]	3.32 ± 0.06	5.19 ± 0.26	20.09 ± 0.27	29.3 ± 0.7	4.09 ± 0.06	2.43 ± 0.04	1.82 ± 0.16
	*2854[a]	3.35 ± 0.12	4.70 ± 0.69	19.92 ± 1.61	27.8 ± 2.3	4.04 ± 0.15	2.37 ± 0.12	-
	*2854ᵦ[a]	3.32 ± 0.06	5.12 ± 0.25	20.71 ± 0.28	29.5 ± 0.7	4.10 ± 0.06	2.45 ± 0.04	1.82 ± 0.16
	*2855[a]	3.60 ± 0.08	5.14 ± 0.42	18.77 ± 0.69	28.2 ± 1.3	4.27 ± 0.10	2.42 ± 0.06	-
	*2855ᵦ[a]	3.26 ± 0.06	5.89 ± 0.29	21.03 ± 0.29	31.9 ± 0.8	4.17 ± 0.06	2.54 ± 0.04	1.86 ± 0.16
	*2856[a]	3.33 ± 0.13	5.81 ± 0.83	20.47 ± 1.60	31.3 ± 2.6	4.20 ± 0.17	2.52 ± 0.13	-
	*2856ᵦ[a]	3.23 ± 0.06	6.36 ± 0.33	20.87 ± 0.29	33.1 ± 1.0	4.21 ± 0.07	2.58 ± 0.04	2.01 ± 0.18
	*2857[a]	3.49 ± 0.09	5.30 ± 0.46	18.88 ± 0.81	28.7 ± 1.4	4.21 ± 0.10	2.42 ± 0.07	-
	*2857ᵦ[a]	3.19 ± 0.05	6.55 ± 0.33	20.36 ± 0.28	33.3 ± 0.9	4.19 ± 0.07	2.57 ± 0.04	1.80 ± 0.16
	*2858[a]	3.21 ± 0.12	5.51 ± 0.76	22.36 ± 1.64	31.8 ± 2.4	4.11 ± 0.15	2.56 ± 0.12	1.83 ± 0.16
	*2858ᵦ[a]	3.22 ± 0.06	5.02 ± 0.24	19.09 ± 0.26	28.1 ± 0.7	3.96 ± 0.06	2.34 ± 0.03	1.83 ± 0.16
				Nine Storey Palace Temple, Kathmandu				
2018	132[a]	3.15 ± 0.21	3.06 ± 0.18	15.41 ± 0.65	19.8 ± 0.7	2.97 ± 0.16	1.84 ± 0.06	1.42 ± 0.08
	133[a]	3.01 ± 0.19	3.85 ± 0.18	8.58 ± 0.39	17.0 ± 0.6	2.83 ± 0.15	1.58 ± 0.05	1.38 ± 0.08
	134[a]	3.01 ± 0.20	4.28 ± 0.19	9.12 ± 0.44	18.6 ± 0.6	2.89 ± 0.16	1.65 ± 0.06	1.49 ± 0.07
	135[a]	3.45 ± 0.21	3.30 ± 0.15	7.38 ± 0.33	14.6 ± 0.5	3.05 ± 0.17	1.56 ± 0.06	1.41 ± 0.05
	136[a]	2.98 ± 0.19	2.13 ± 0.13	8.38 ± 0.39	12.0 ± 0.5	2.59 ± 0.15	1.36 ± 0.05	1.34 ± 0.06
				Pashupati Temple, Kathmandu				
'18	235[a]	3.59 ± 0.30	4.71 ± 0.26	11.07 ± 0.62	21.3 ± 0.9	3.50 ± 0.24	1.95 ± 0.08	1.52 ± 0.12
	236[a]	3.63 ± 0.29	4.61 ± 0.23	11.76 ± 0.63	21.6 ± 0.8	3.53 ± 0.24	1.98 ± 0.08	1.67 ± 0.15
				Trailokya Mohan Temple, Kathmandu				
'18	237[a]	3.12 ± 0.26	3.68 ± 0.22	8.43 ± 0.50	16.5 ± 0.7	2.96 ± 0.21	1.59 ± 0.07	1.27 ± 0.26

Table S2: Equivalent concentrations of K, U and Th determined by HRGS[a] and ICPMS[b], converted to alpha, beta and gamma dose rates based on conversion factors in Guerin et al. (2011)[c], together with the gamma dose rates measured in the field[d]

Year	Lab code	Water content /%	Effective Beta dose rate[e]	Effective Gamma dose rate[f]	Cosmic dose contribution[g]	Total effective dose rate
			/ mGy a^{-1}			
Changu Narayan Temple, Bhaktapur						
2018	229	17 ± 4	2.54 ± 0.19	1.67 ± 0.11	0.19 ± 0.02	4.40 ± 0.22
	230	23 ± 4	2.39 ± 0.18	1.66 ± 0.09	0.19 ± 0.02	4.24 ± 0.20
	231	25 ± 7	2.33 ± 0.21	1.52 ± 0.11	0.20 ± 0.02	4.04 ± 0.24
Vatsala Temple, Bhaktapur						
'16	*2859	13 ± 4	2.74 ± 0.13	1.68 ± 0.17	0.11 ± 0.01	4.46 ± 0.21
	*2860	13 ± 4	2.75 ± 0.14	1.80 ± 0.20	0.10 ± 0.01	4.56 ± 0.24
Jaisideval Temple, Kathmandu						
2018	232	16 ± 3	2.70 ± 0.21	1.74 ± 0.17	0.15 ± 0.02	4.59 ± 0.27
	233	26 ± 3	2.83 ± 0.18	1.75 ± 0.15	0.15 ± 0.02	4.73 ± 0.24
	234	20 ± 6	2.38 ± 0.22	1.11 ± 0.08	0.19 ± 0.02	3.68 ± 0.24
2017	74	19 ± 3	2.98 ± 0.07	2.04 ± 0.10	0.15 ± 0.02	5.18 ± 0.12
	75	11 ± 3	3.99 ± 0.10	2.26 ± 0.11	0.15 ± 0.02	6.40 ± 0.14
	76	9 ± 5	3.39 ± 0.09	1.86 ± 0.10	0.15 ± 0.02	5.40 ± 0.13
Kasthamandap Temple, Kathmandu						
'17	77	18 ± 3	4.02 ± 0.09	2.87 ± 0.14	0.19 ± 0.02	7.08 ± 0.15
2016	*2851	18 ± 2	3.06 ± 0.07[e]	2.02 ± 0.19	0.12 ± 0.01	5.20 ± 0.20
	*2852	11 ± 4	3.67 ± 0.18[e]	2.23 ± 0.22	0.12 ± 0.01	6.02 ± 0.29
	*2853	13 ± 5	3.31 ± 0.19[e]	1.97 ± 0.19	0.15 ± 0.02	5.44 ± 0.27
	*2854	11 ± 3	3.40 ± 0.14[e]	2.04 ± 0.21	0.12 ± 0.01	5.57 ± 0.25
	*2855	13 ± 4	3.36 ± 0.16[e]	2.07 ± 0.21	0.12 ± 0.01	5.55 ± 0.26
	*2856	13 ± 4	3.47 ± 0.17[e]	2.16 ± 0.25	0.11 ± 0.01	5.74 ± 0.30
	*2857	13 ± 4	3.38 ± 0.16[e]	2.05 ± 0.21	0.11 ± 0.01	5.54 ± 0.26
	*2858	13 ± 4	3.21 ± 0.15[e]	2.03 ± 0.25	0.12 ± 0.01	5.36 ± 0.29
Nine Storey Temple, Kathmandu						
2017	133	20 ± 5	2.31 ± 0.17	1.33 ± 0.11	0.17 ± 0.02	3.81 ± 0.18
	134	20 ± 5	2.36 ± 0.17	1.42 ± 0.10	0.17 ± 0.02	3.94 ± 0.19
	136	20 ± 5	2.11 ± 0.16	1.22 ± 0.09	0.21 ± 0.02	3.55 ± 0.17
Pashupati Temple, Kathmandu						
'18	235	17 ± 4	2.93 ± 0.23	1.52 ± 0.12	0.15 ± 0.01	4.60 ± 0.26
	236	16 ± 6	3.00 ± 0.28	1.67 ± 0.15	0.15 ± 0.01	4.82 ± 0.32
Trailokya Mohan Temple, Kathmandu						
'18	237	18 ± 3	2.47 ± 0.19	1.27 ± 0.26	0.13 ± 0.01	3.86 ± 0.32

Table S3: Total effective environmental dose rates to HF-etched 200 μm quartz following water correction and inverse grain size attenuation; [e] combining dry beta dose rates from TSBC and HRGS; [f] combining gamma dose rate estimates from HRGS and ICPMS and wet gamma dose rates measured in the field; [g]cosmic dose contributions calculated from Prescott and Hutton (1994) combining latitude and altitude specific dose rates with corrections for estimated depth of overburden

Lab code	Field ID	Age / ka	Age / Calendar years
CERSA136	Nine Storey, NDT Tr3 [19]	0.43 ± 0.07	AD 1590 ± 70
CERSA074	Jaisideval, JSD16, AT5/6 [2196]	0.50 ± 0.06	AD1520 ± 60
CERSA232	Jaisideval, JSF17-1 Tr3	0.54 ± 0.01	AD 1480 ± 70
CERSA133	Nine Storey, NDT Tr3 [10, cut]	0.58 ± 0.07	AD 1440 ± 70
CERSA234	Jaisideval, JSF17-3 Tr3	0.65 ± 0.01	AD 1340 ± 200
CERSA134	Nine Storey, NDT Tr3 [10, base]	0.68 ± 0.04	AD 1330 ± 40
CERSA075	Jaisideval, JSD16, AT3 [2231]	0.96 ±0.06	AD1060 ± 60
CERSA237	Trailokya Mohan, TLM17-1	0.98 ± 0.02	AD 1040 ± 120
CERSA076	Jaisideval, JSD16, AT3 [2198]	1.12 ±0.08	AD900 ± 80
CERSA231	Changu Narayan, CGN17-3	1.27 ± 0.02	AD 750 ± 90
SUTL2858	Kasthamandap, OSL6	1.27 ± 0.05	AD 750 ± 60
SUTL2856	Kasthamandap, OSL4	1.35 ± 0.08	AD 660 ± 200
CERSA230	Changu Narayan, CGN17-2	1.39 ± 0.02	AD 630 ± 90
SUTL2854	Kasthamandap, OSL2	1.39 ± 0.16	AD 630 ± 160
CERSA235	Pashupati PASH17-1 Tr5	1.50 ± 0.02	AD 520 ± 120
SUTL2855	Kasthamandap, OSL3	1.55 ± 0.14	AD 470 ± 140
CERSA077	Kasthamandap, HMD16, M5 [1286]	1.92 ±0.09	AD100 ± 90
SUTL2852	Kasthamandap, OSL Env 4	1.91 ± 0.09	AD 100 ± 150
SUTL2857	Kasthamandap, OSL5	2.10 ± 0.07	80 ± 70 BC
SUTL2860	Vatsala OSL2	2.10 ± 0.08	80 ± 80 BC
SUTL2853	Kasthamandap, OSL1	2.11 ± 0.02	100 ± 80 BC
SUTL2859	Vatsala OSL1	2.79 ± 0.10	770 ± 100 BC
SUTL2851	Kasthamandap, OSL Env 2	3.07 ± 0.14	1050 ± 140 BC
CERSA229	Changu Narayan, CGN17-1	3.08 ± 0.09	1060 ± 210 BC
CERSA236	Pashupati PASH17-2 Tr5	3.72 ± 0.04	1700 ± 190 BC
CERSA233	Jaisideval, JSF17-2 Tr3	4.14 ± 0.05	2120 ± 200 BC

Table S4: Quartz OSL SAR sediment ages, re-arranged in Chronological Order

Appendix A

Figure A-1: Apparent 'age' distributions for CERSA229, as (left) a Kernel Density Estimate Plot, and (right) an Abanico Plot
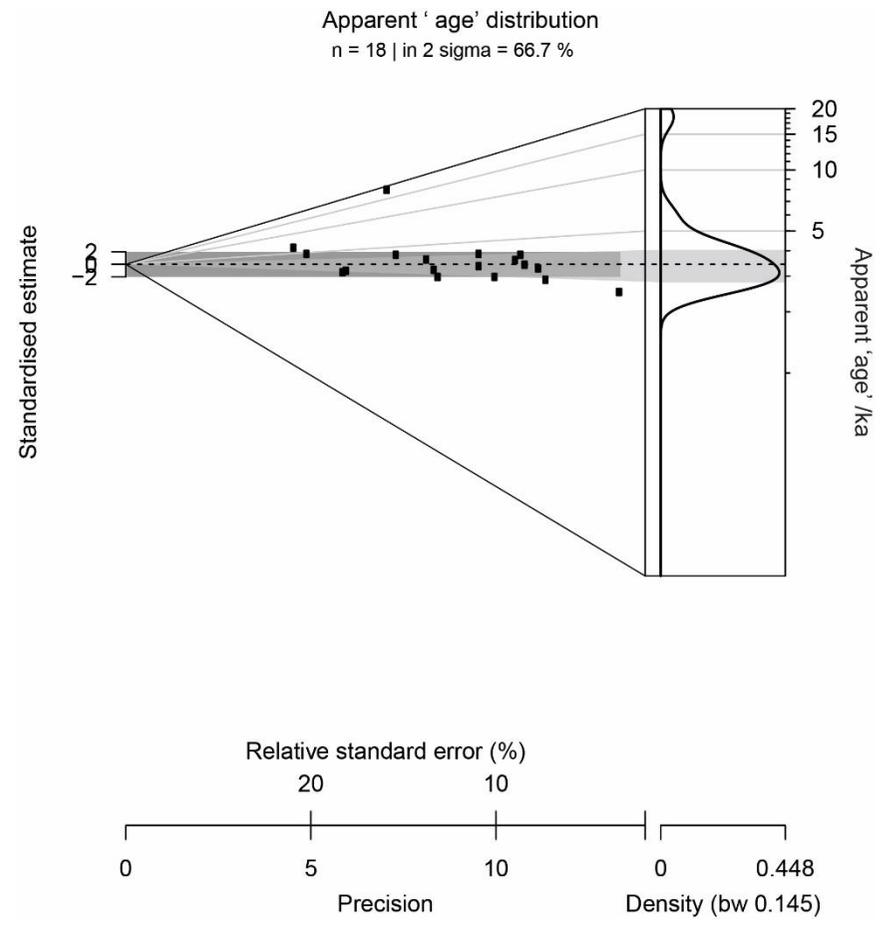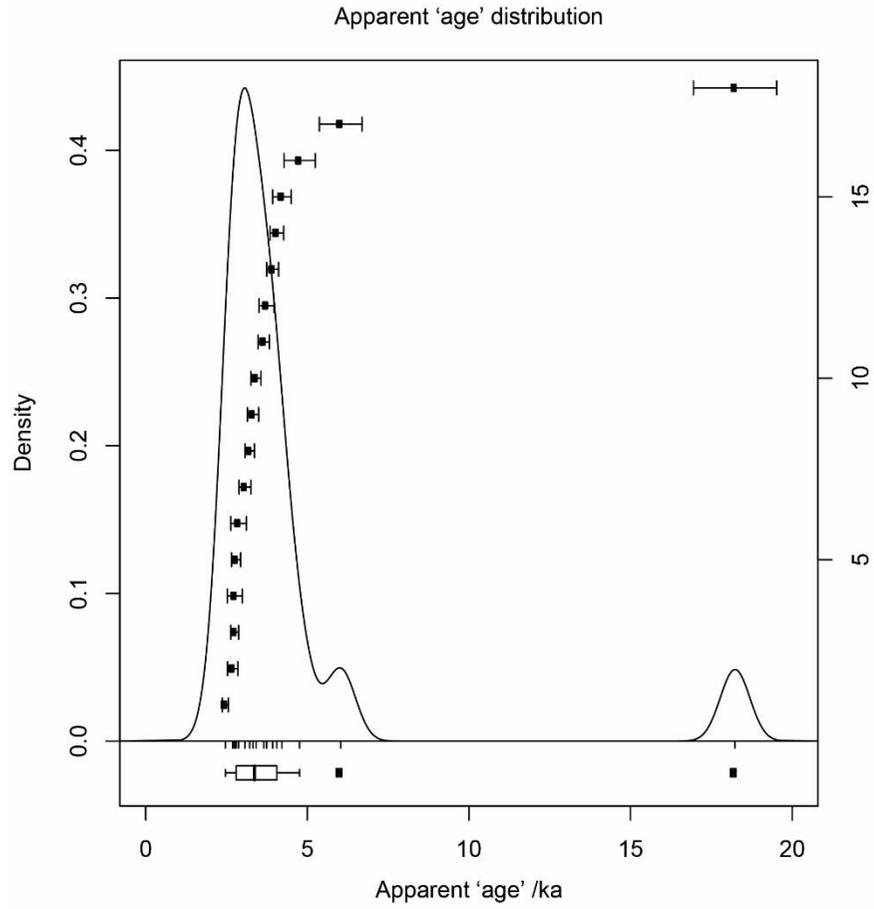
Figure A-2: Apparent 'age' distributions for CERSA230, as (left) a Kernel Density Estimate Plot, and (right) an Abanico Plot
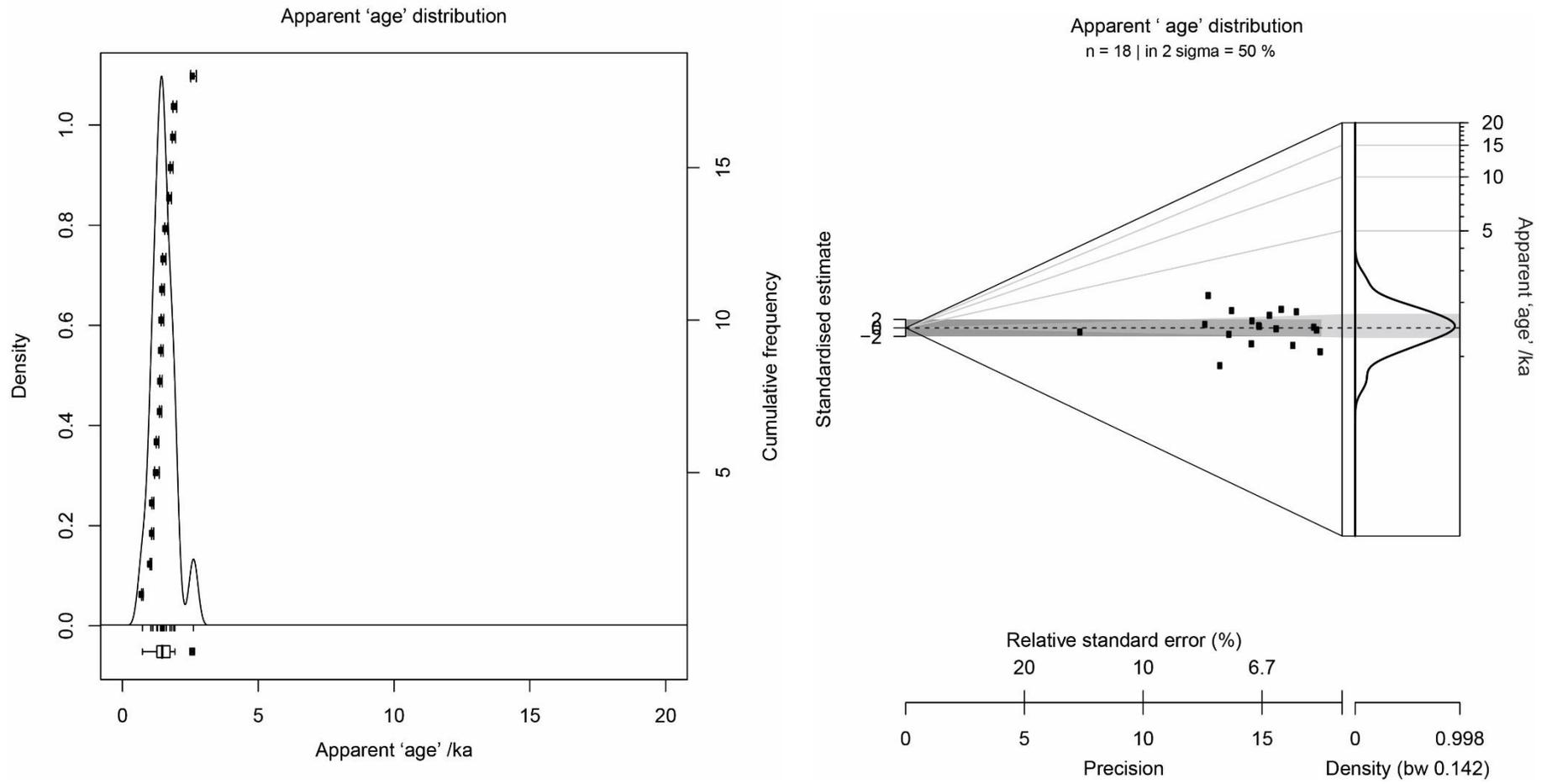
Figure A-3: Apparent 'age' distributions for CERSA231, as (left) a Kernel Density Estimate Plot, and (right) an Abanico Plot
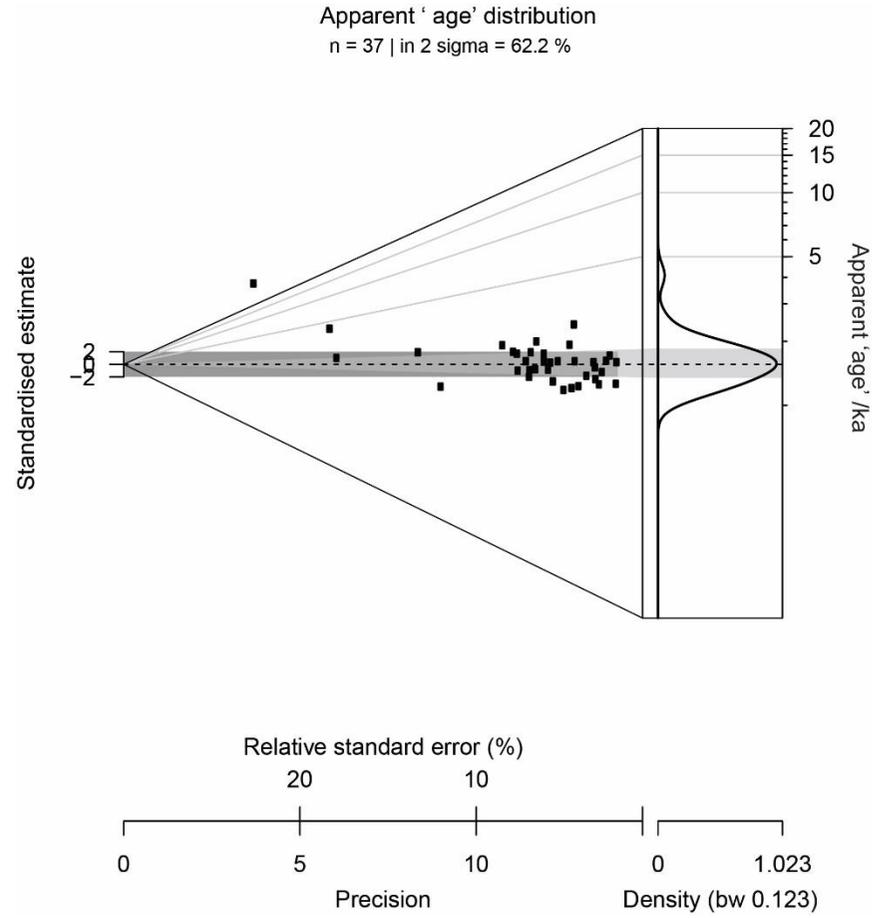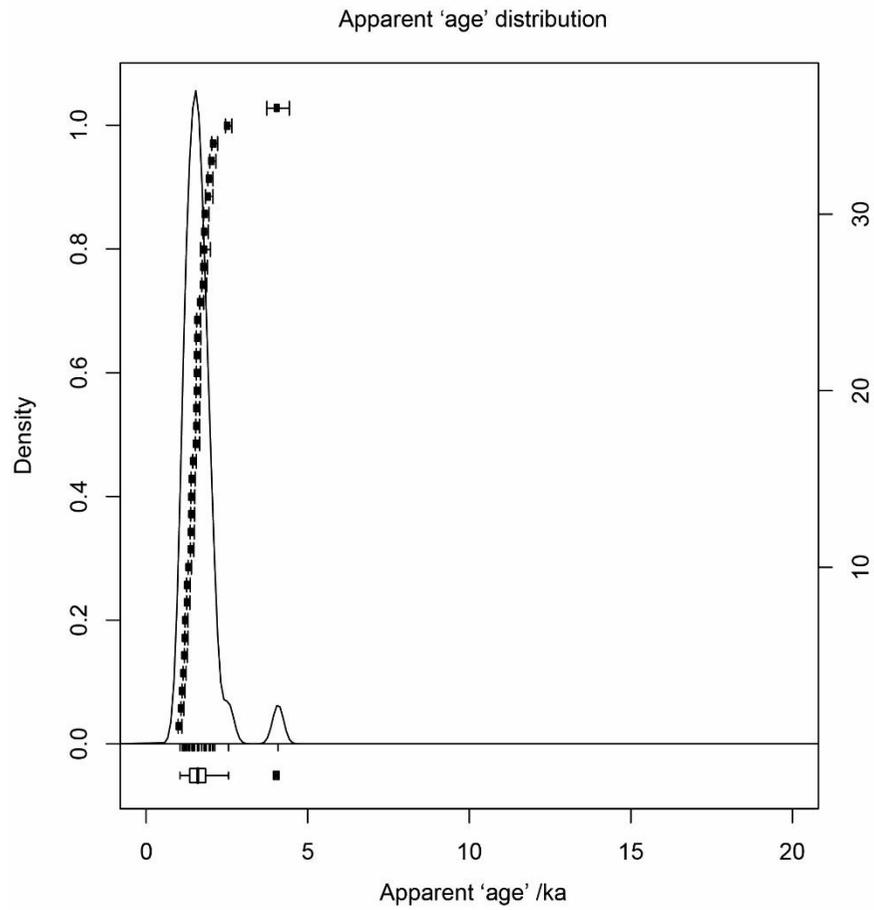
Figure A-4: Apparent 'age' distributions for CERSA232, as (left) a Kernel Density Estimate Plot, and (right) an Abanico Plot
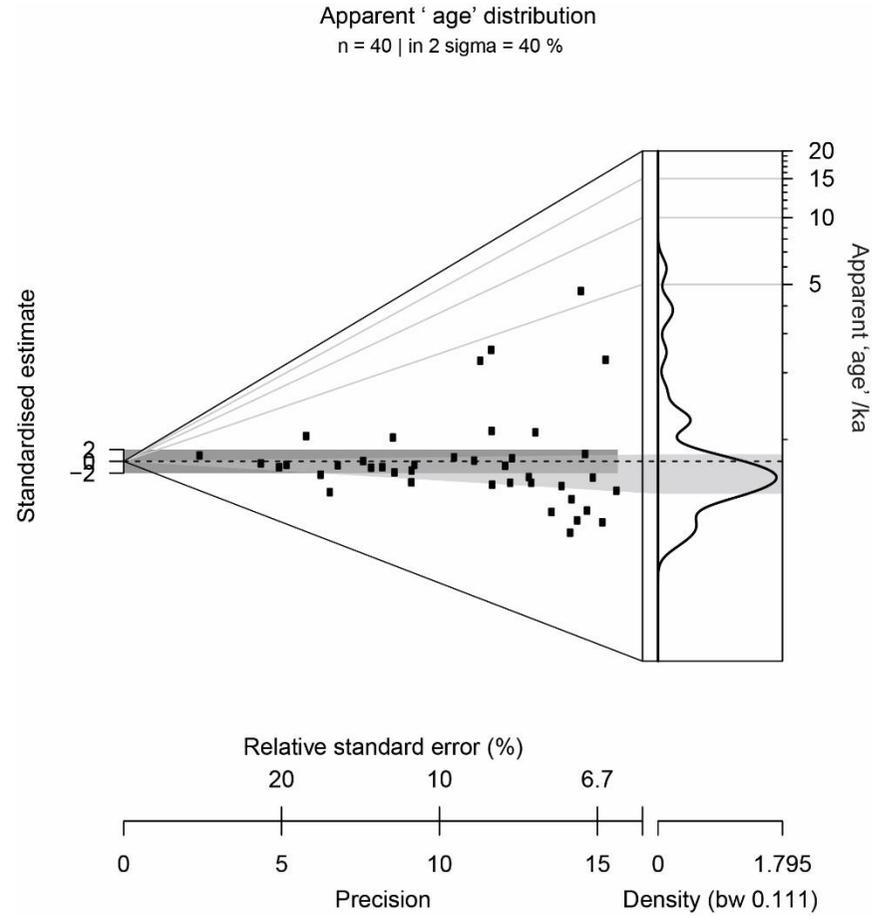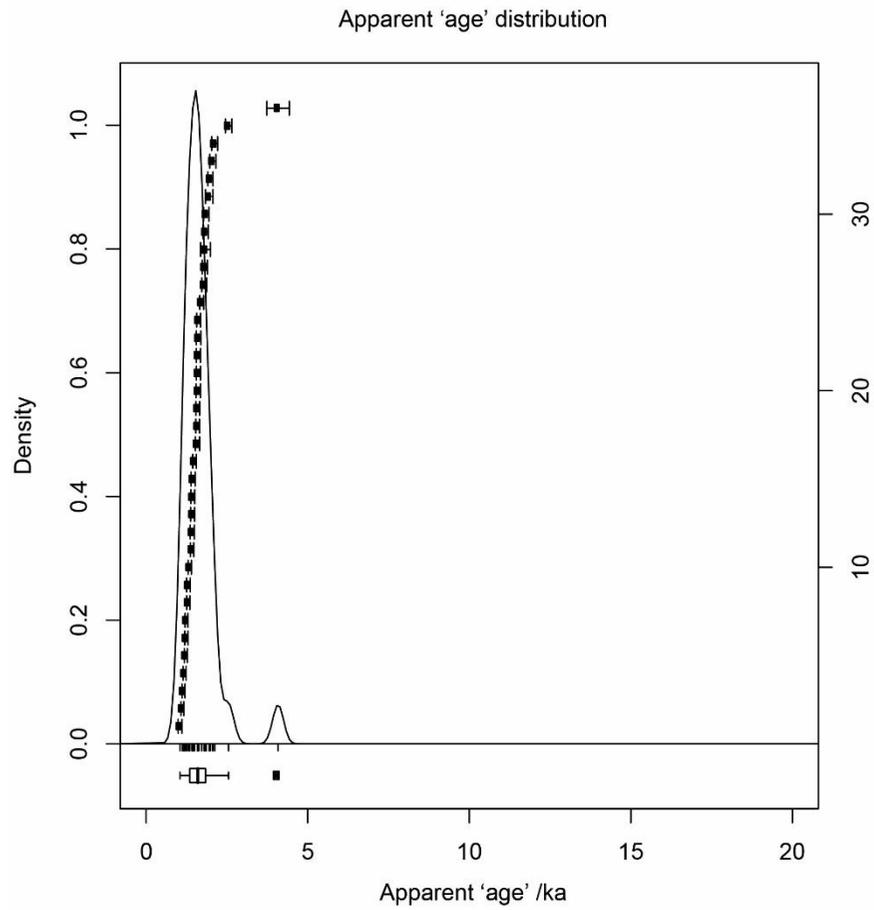
Figure A-5: Apparent 'age' distributions for CERSA233, as (left) a Kernel Density Estimate Plot, and (right) an Abanico Plot
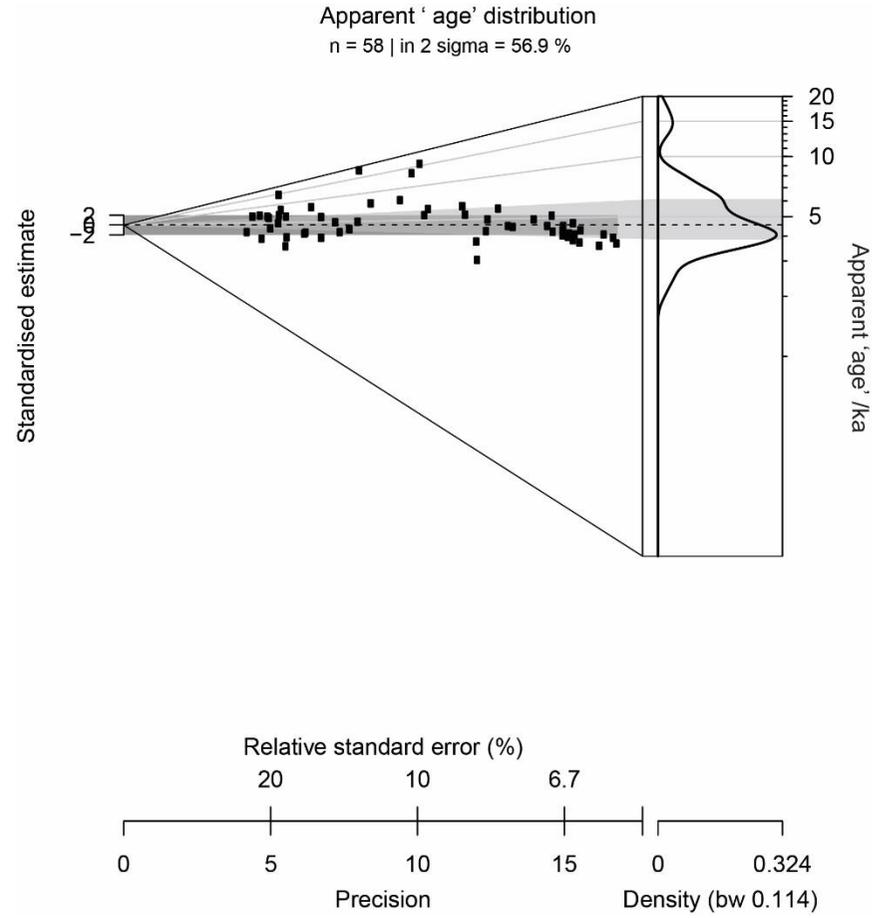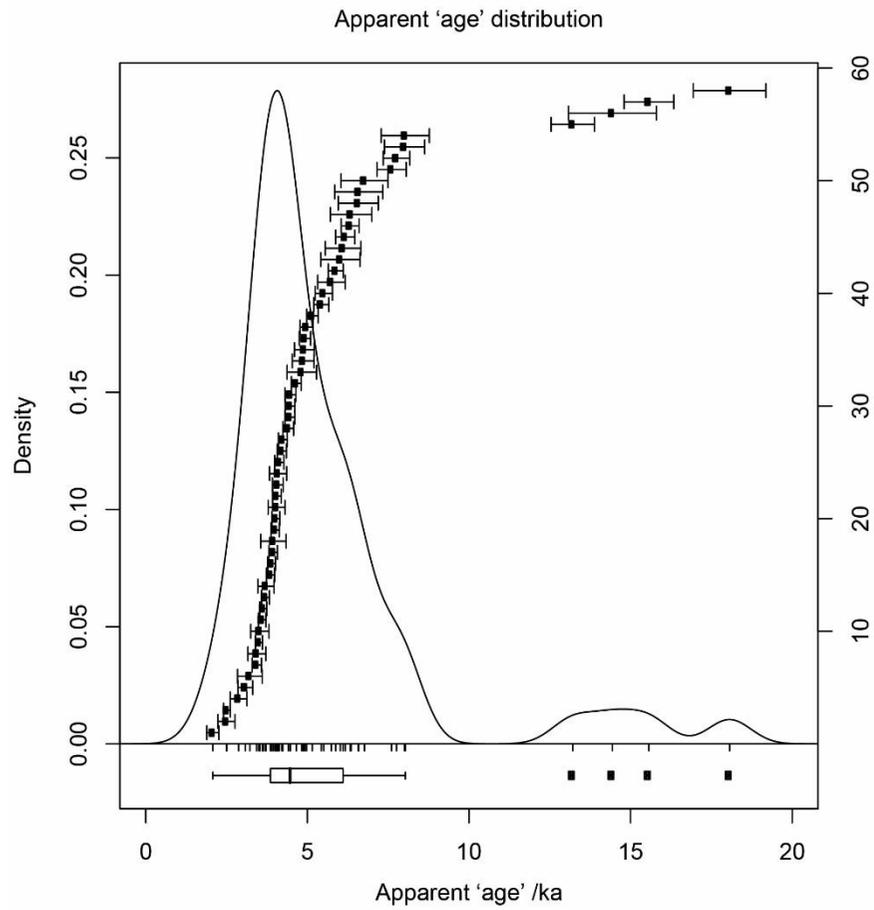
Figure A-6: Apparent 'age' distributions for CERSA234, as (left) a Kernel Density Estimate Plot, and (right) an Abanico Plot
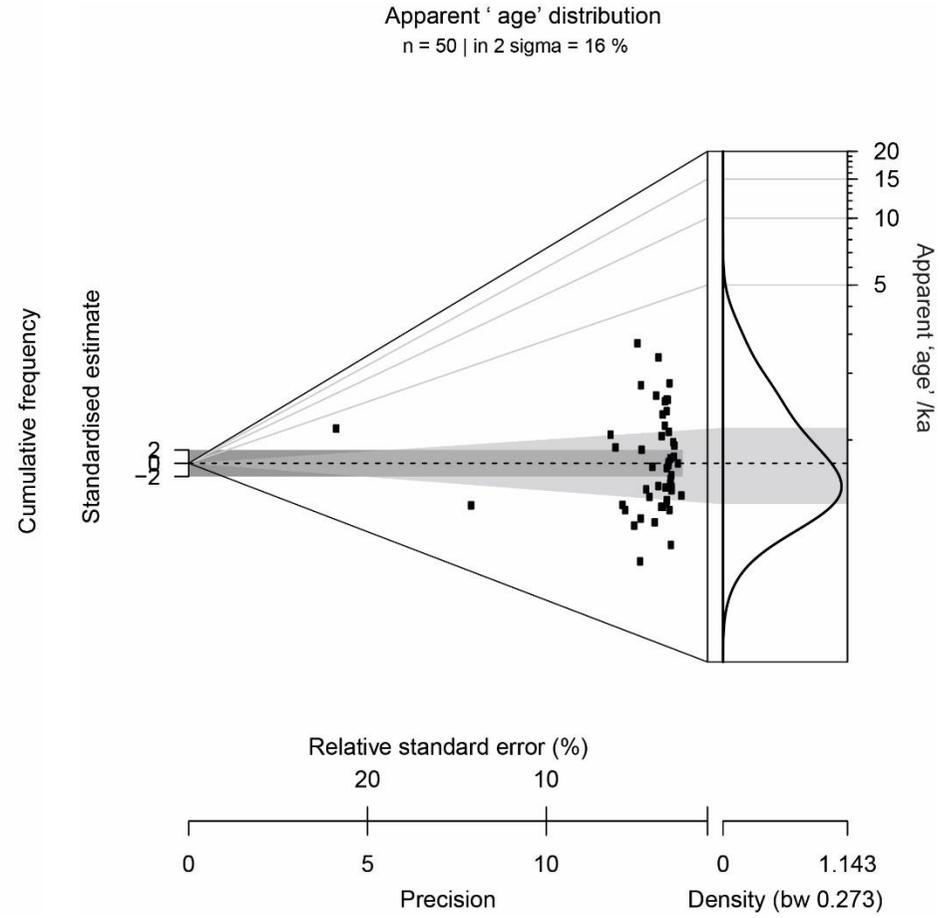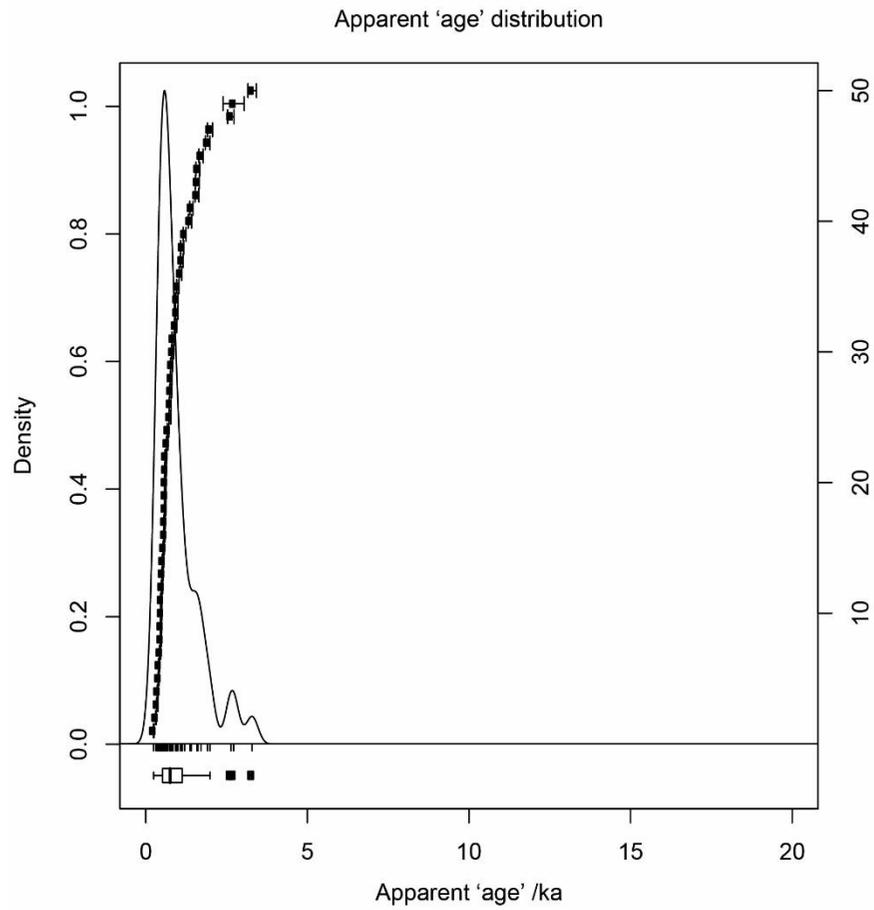
Figure A-7: Apparent 'age' distributions for CERSA074, as (left) a Kernel Density Estimate Plot, and (right) an Abanico Plot
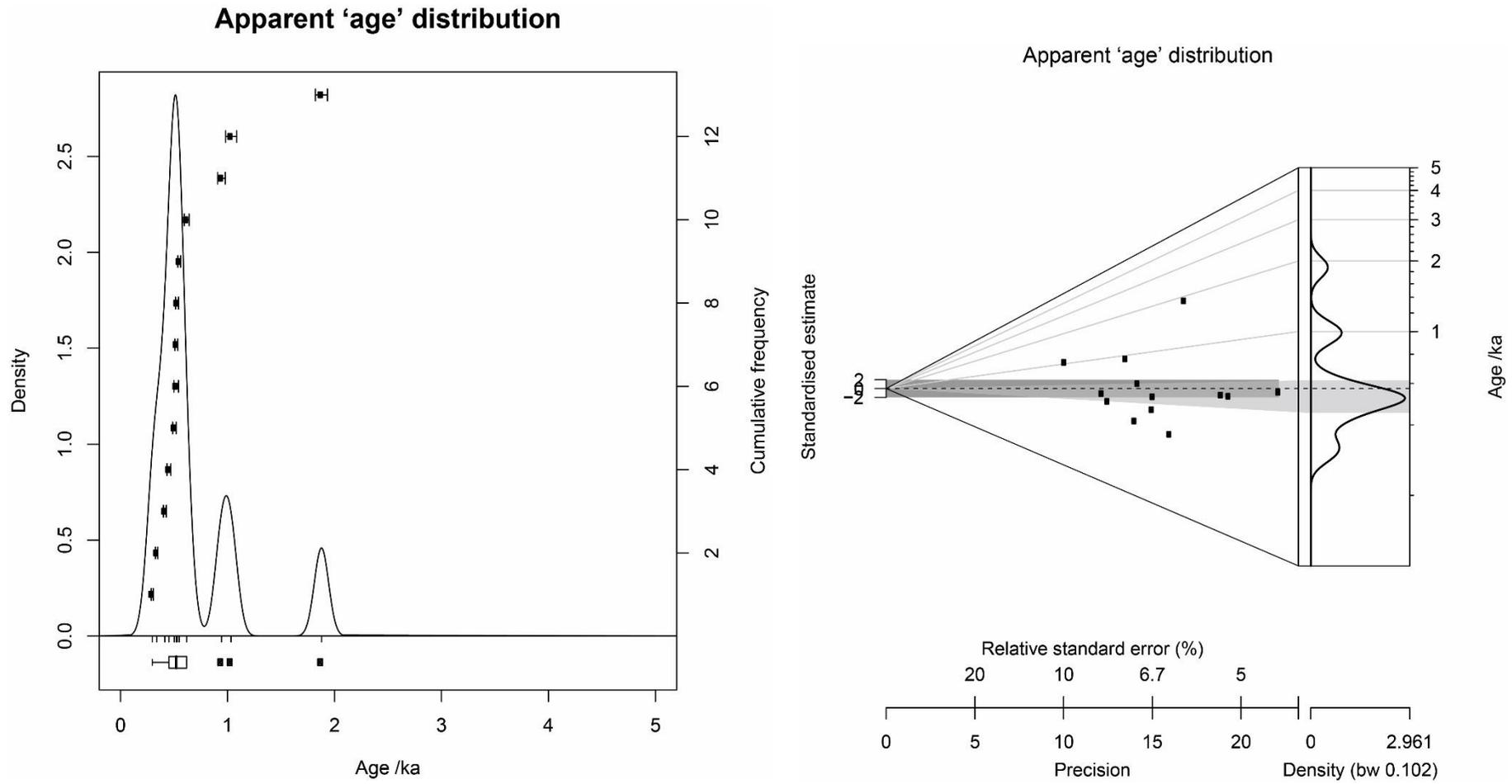
Figure A-8: Apparent 'age' distributions for CERSA075, as (left) a Kernel Density Estimate Plot, and (right) an Abanico Plot
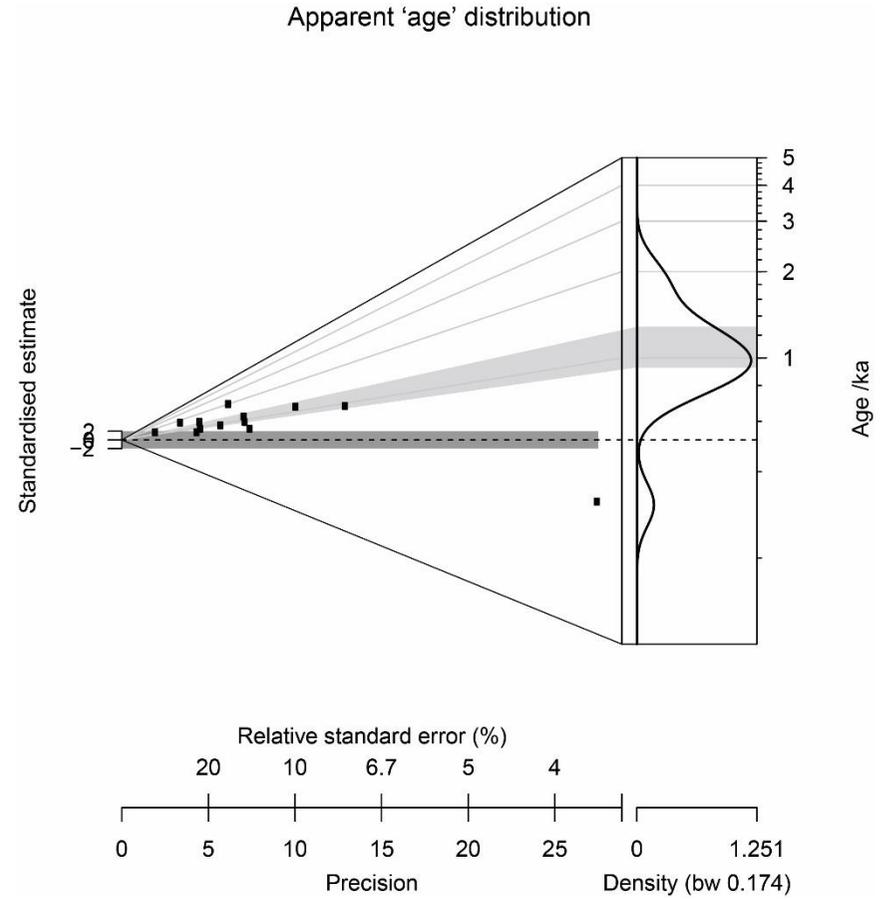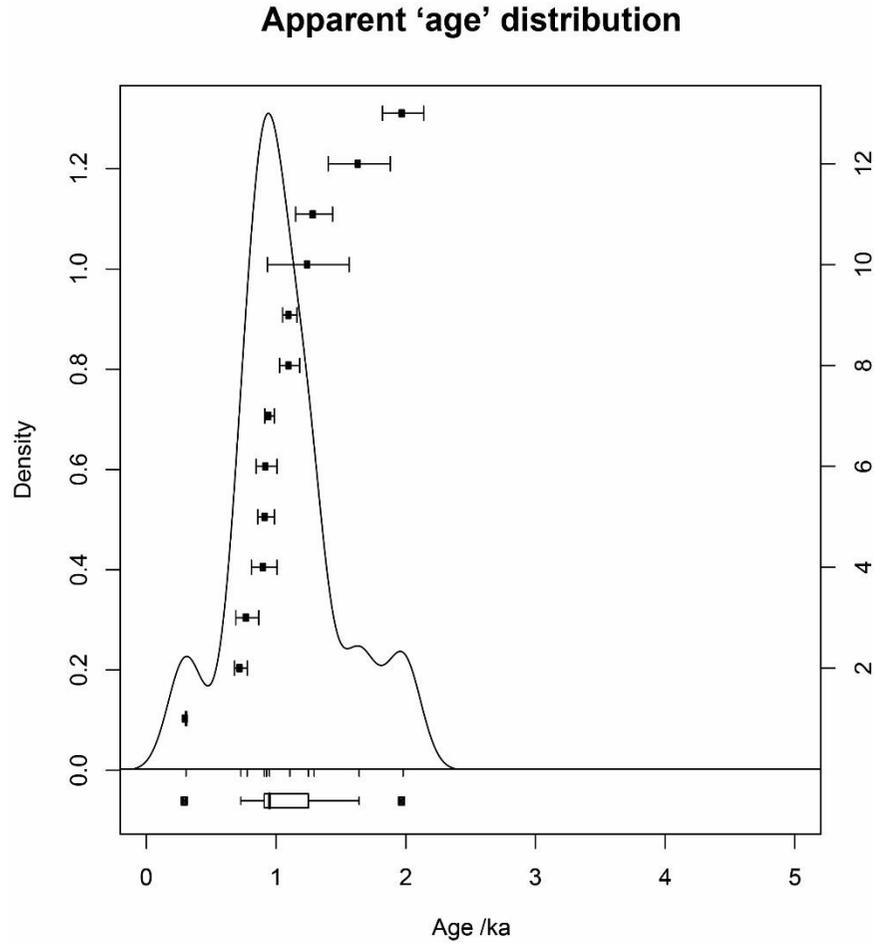
Figure A-9: Apparent 'age' distributions for CERSA076, as (left) a Kernel Density Estimate Plot, and (right) an Abanico Plot
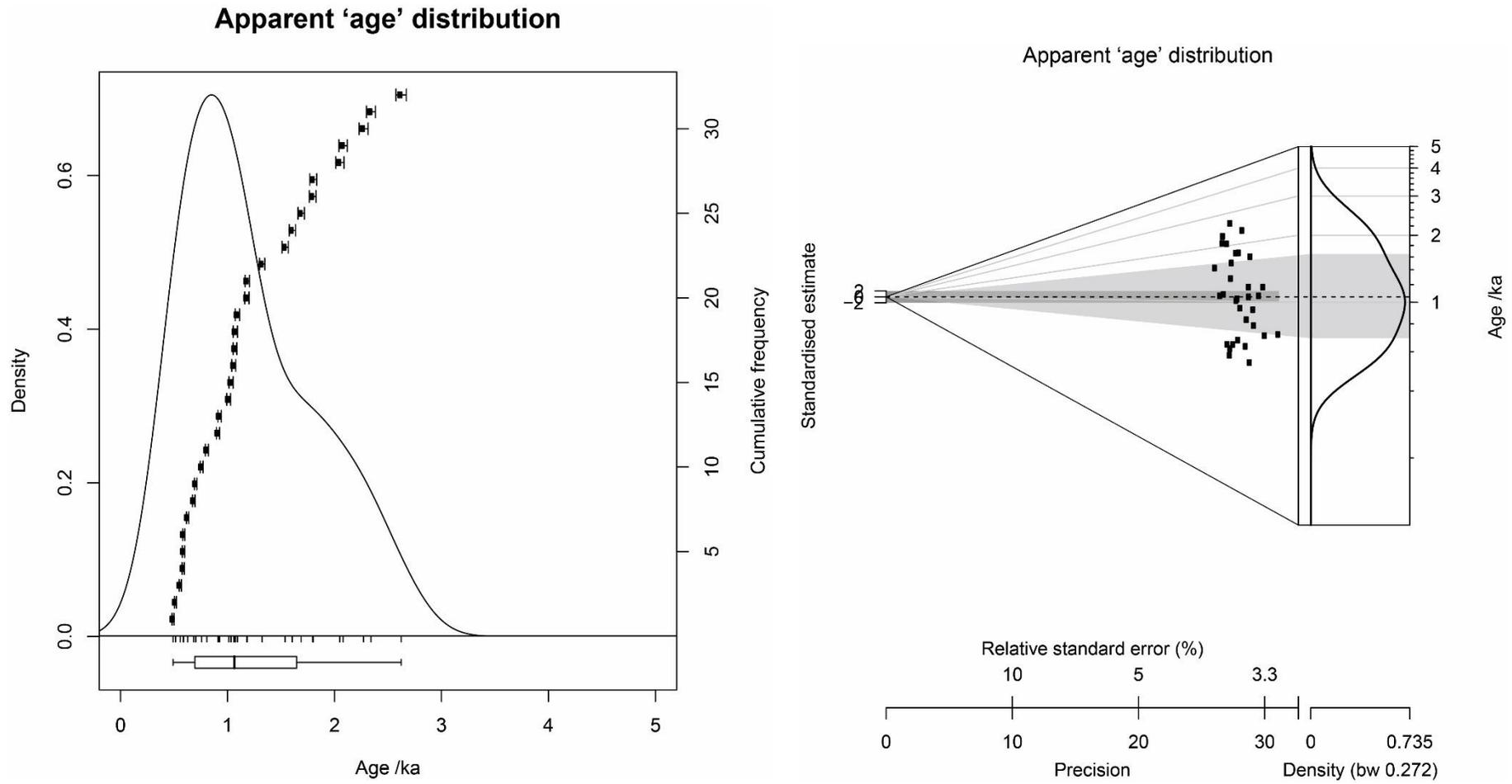
Figure A-10: Apparent 'age' distributions for CERSA077, as (left) a Kernel Density Estimate Plot, and (right) an Abanico Plot
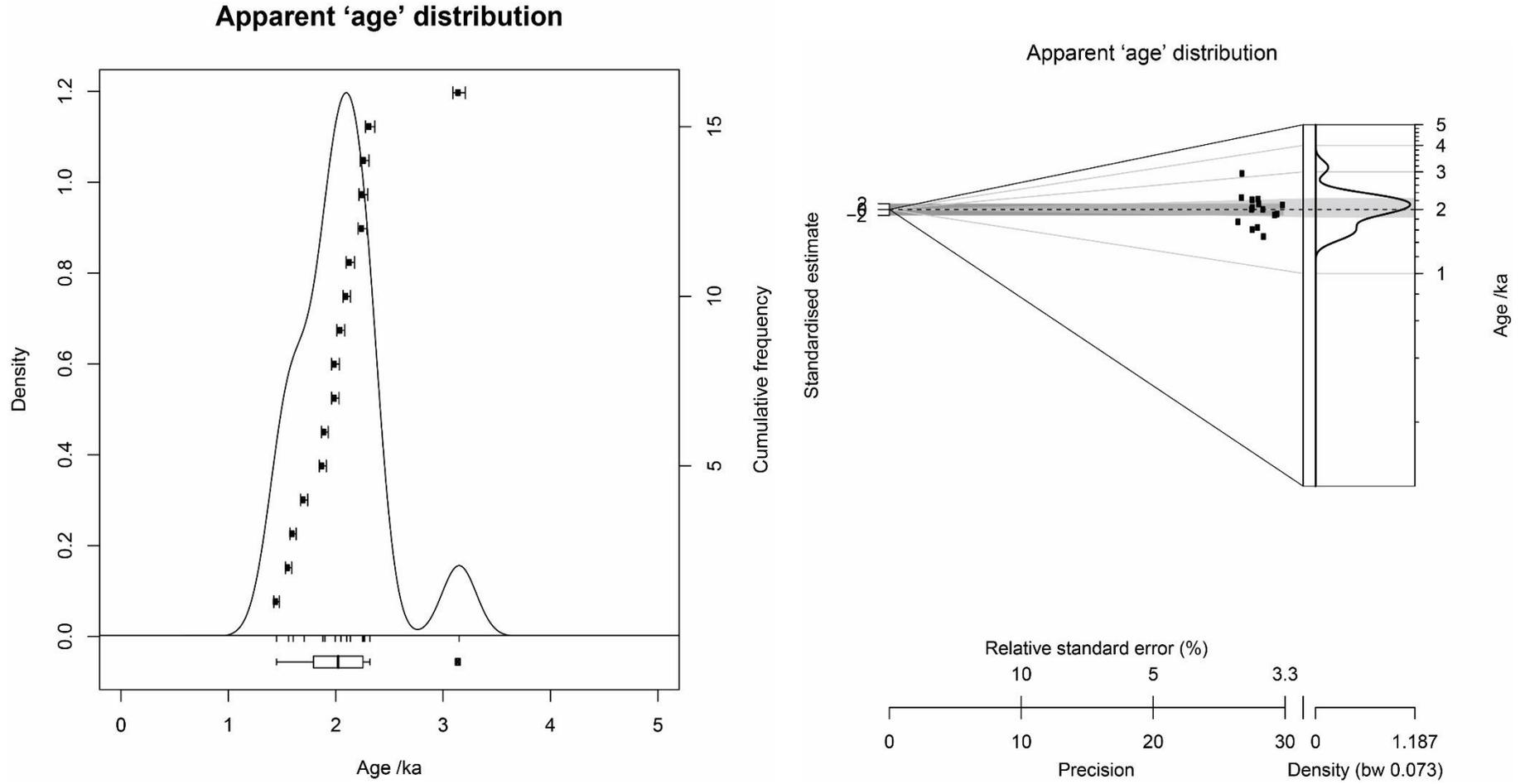
Figure A-11: Apparent 'age' distributions for CERSA133, as (left) a Kernel Density Estimate Plot, and (right) an Abanico Plot
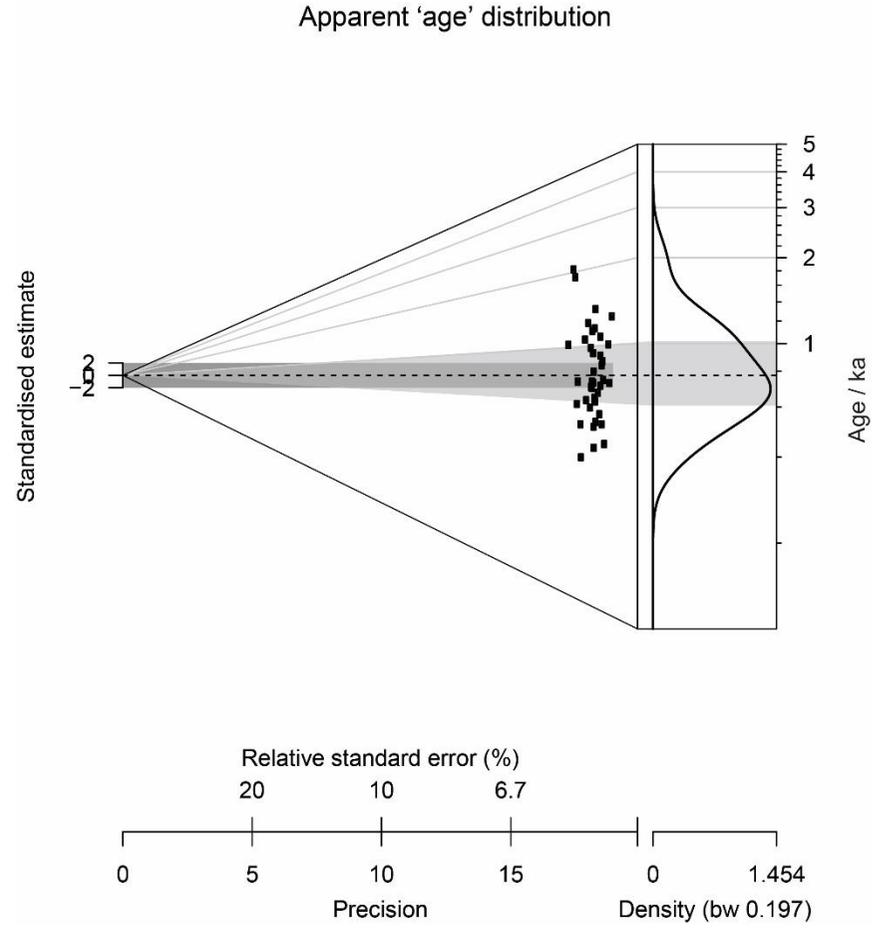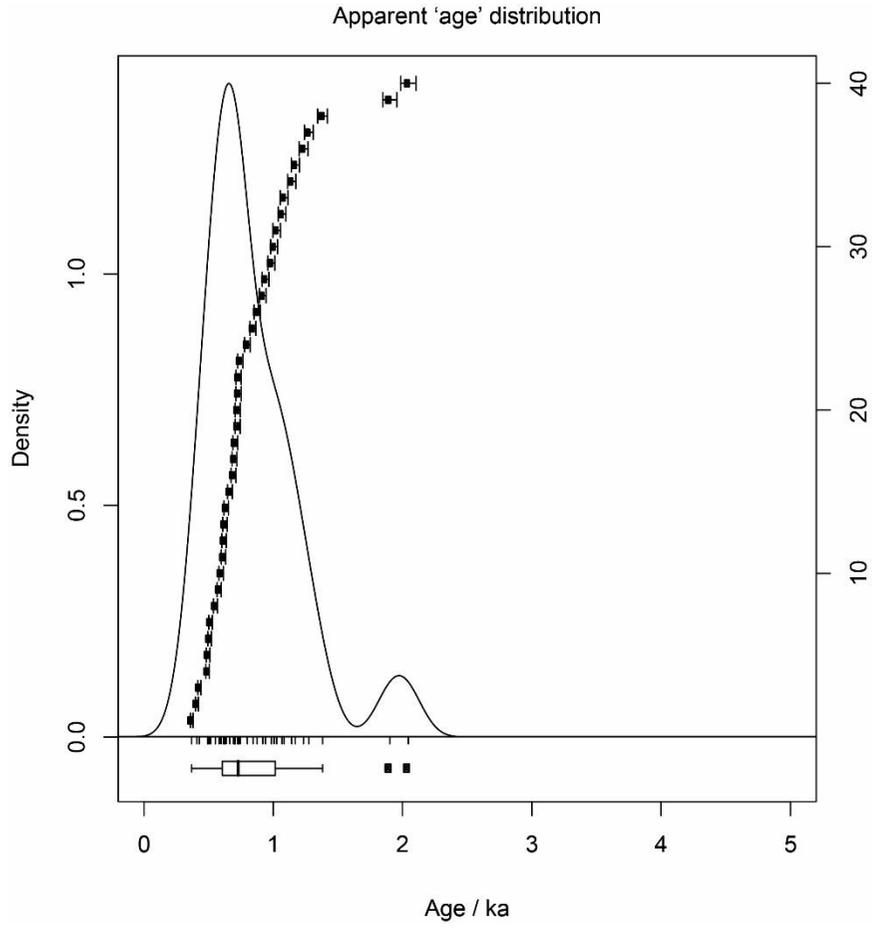
Figure A-12: Apparent 'age' distributions for CERSA134, as (left) a Kernel Density Estimate Plot, and (right) an Abanico Plot
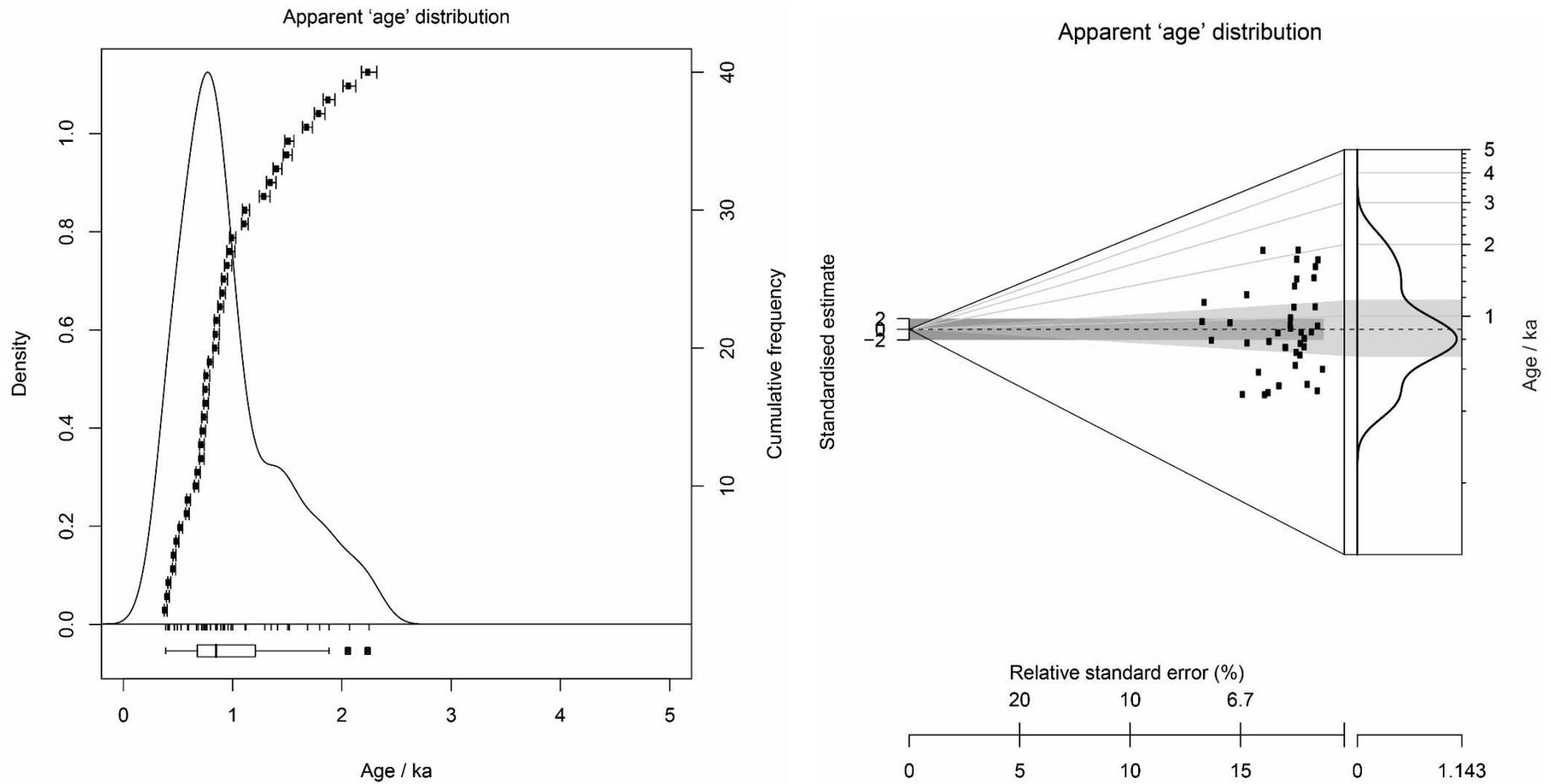
Figure A-13: Apparent 'age' distributions for CERSA136, as (left) a Kernel Density Estimate Plot, and (right) an Abanico Plot
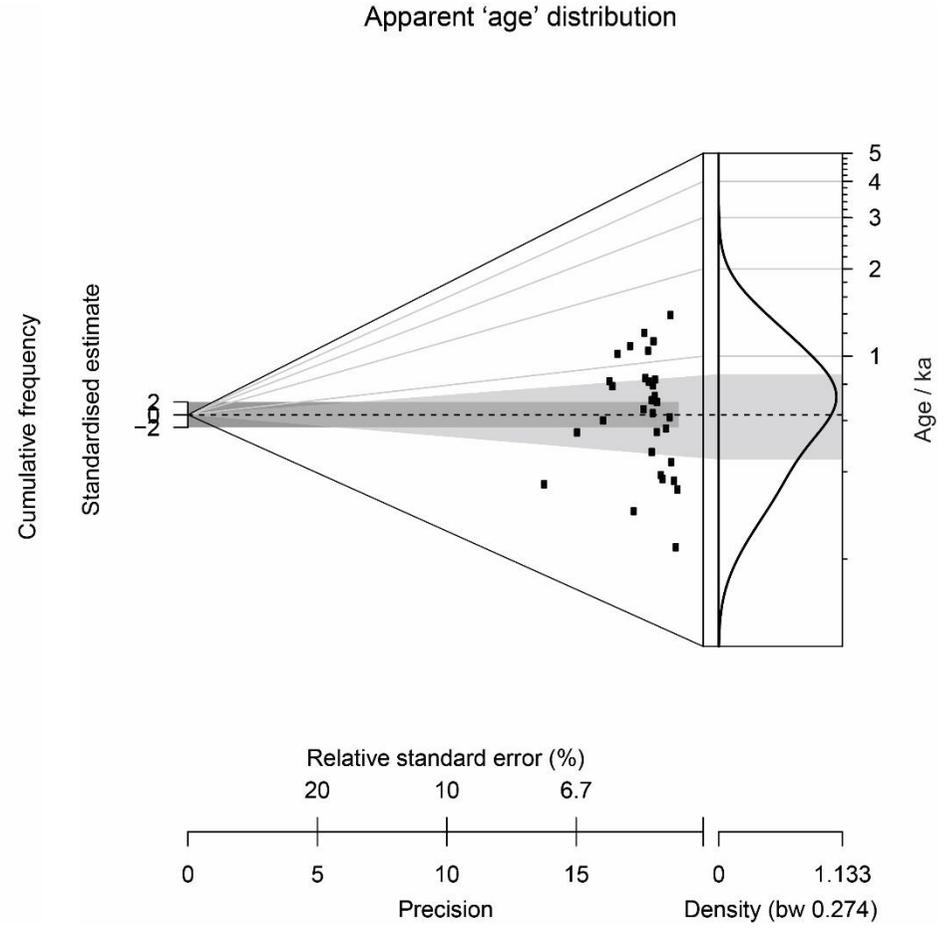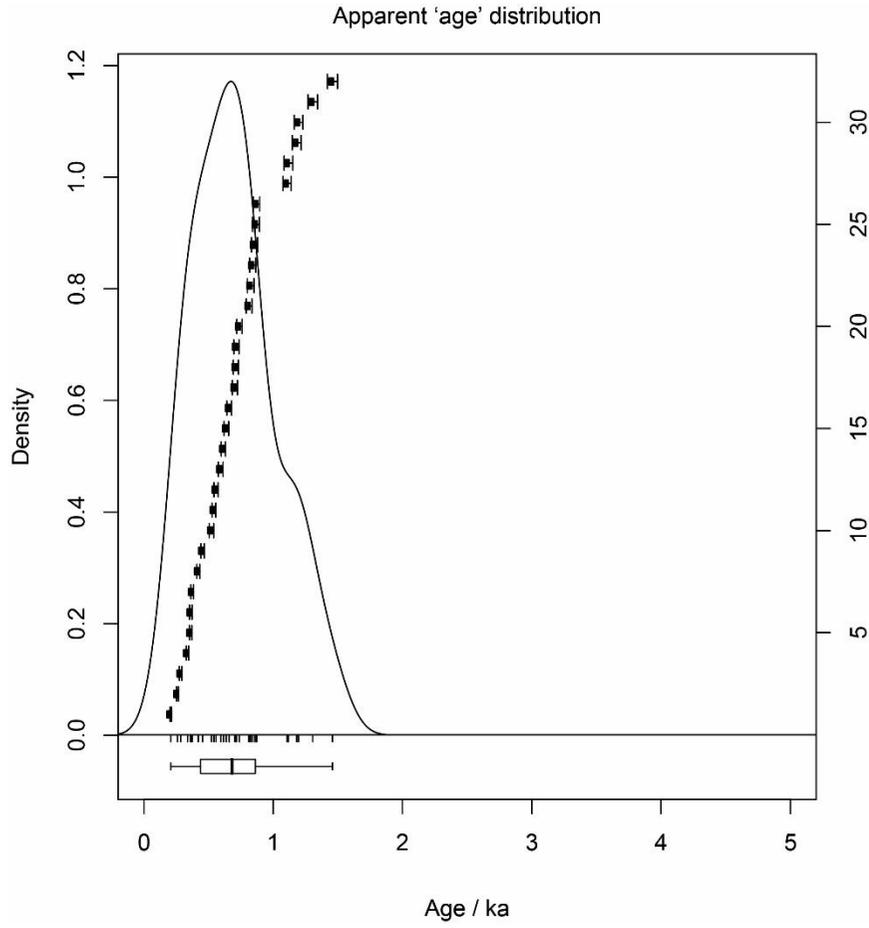
Figure A-14: Apparent 'age' distributions for CERSA235, as (left) a Kernel Density Estimate Plot, and (right) an Abanico Plot
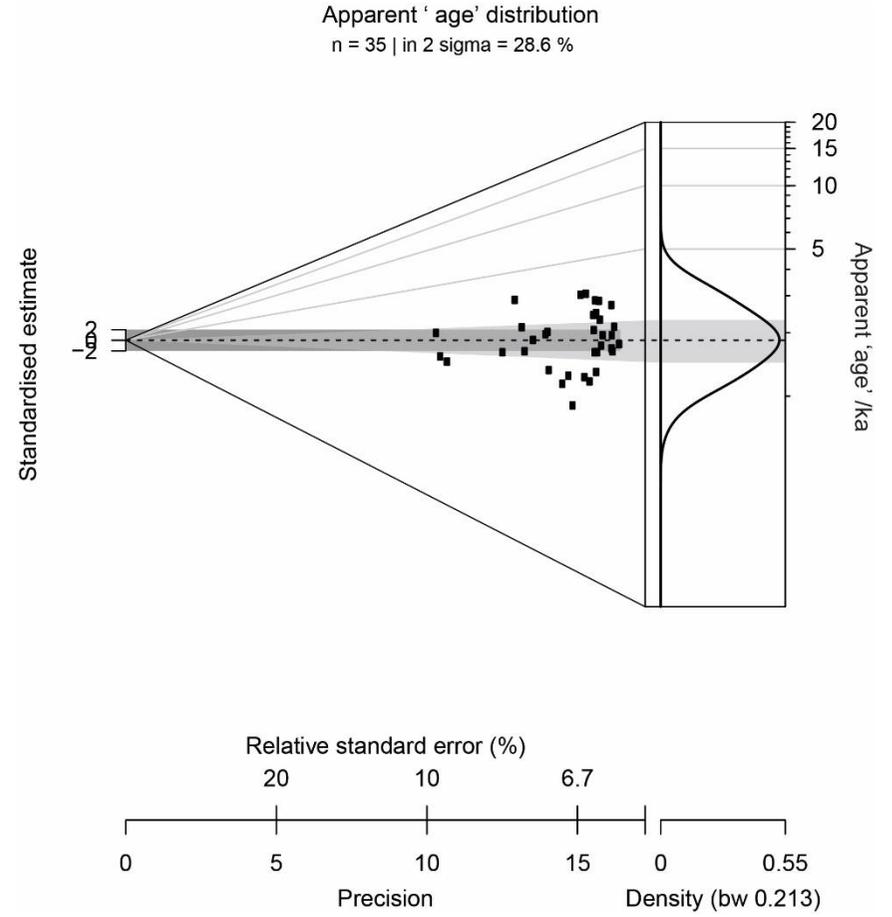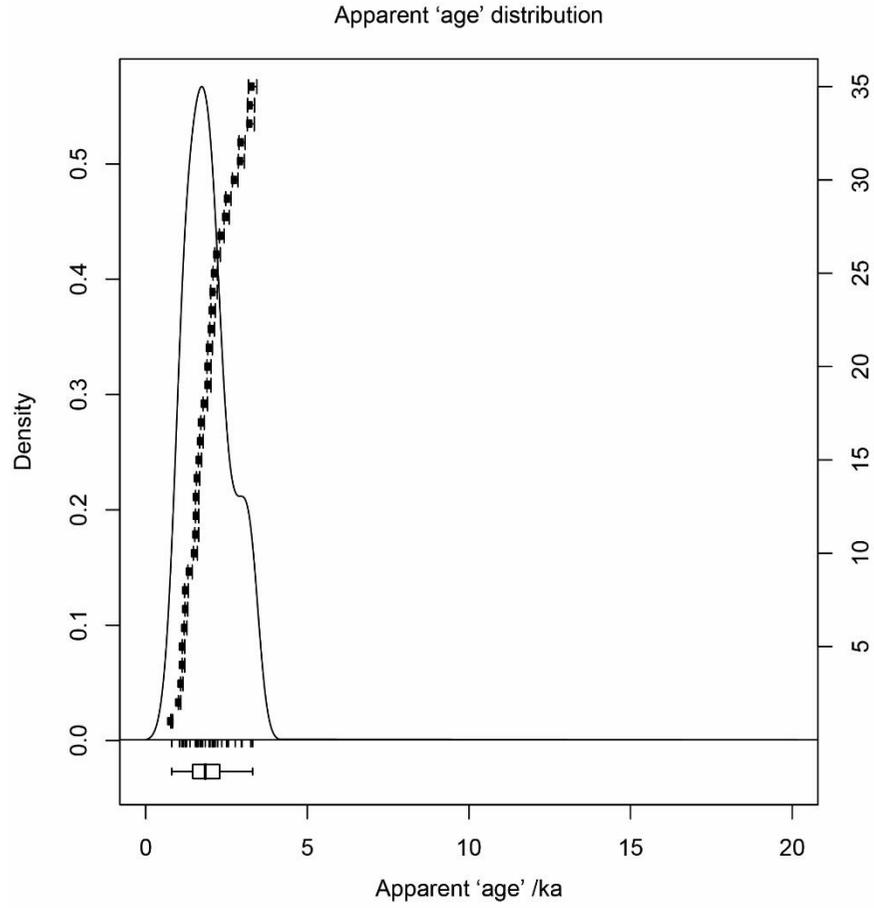
Figure A-15: Apparent 'age' distributions for CERSA236, as (left) a Kernel Density Estimate Plot, and (right) an Abanico Plot
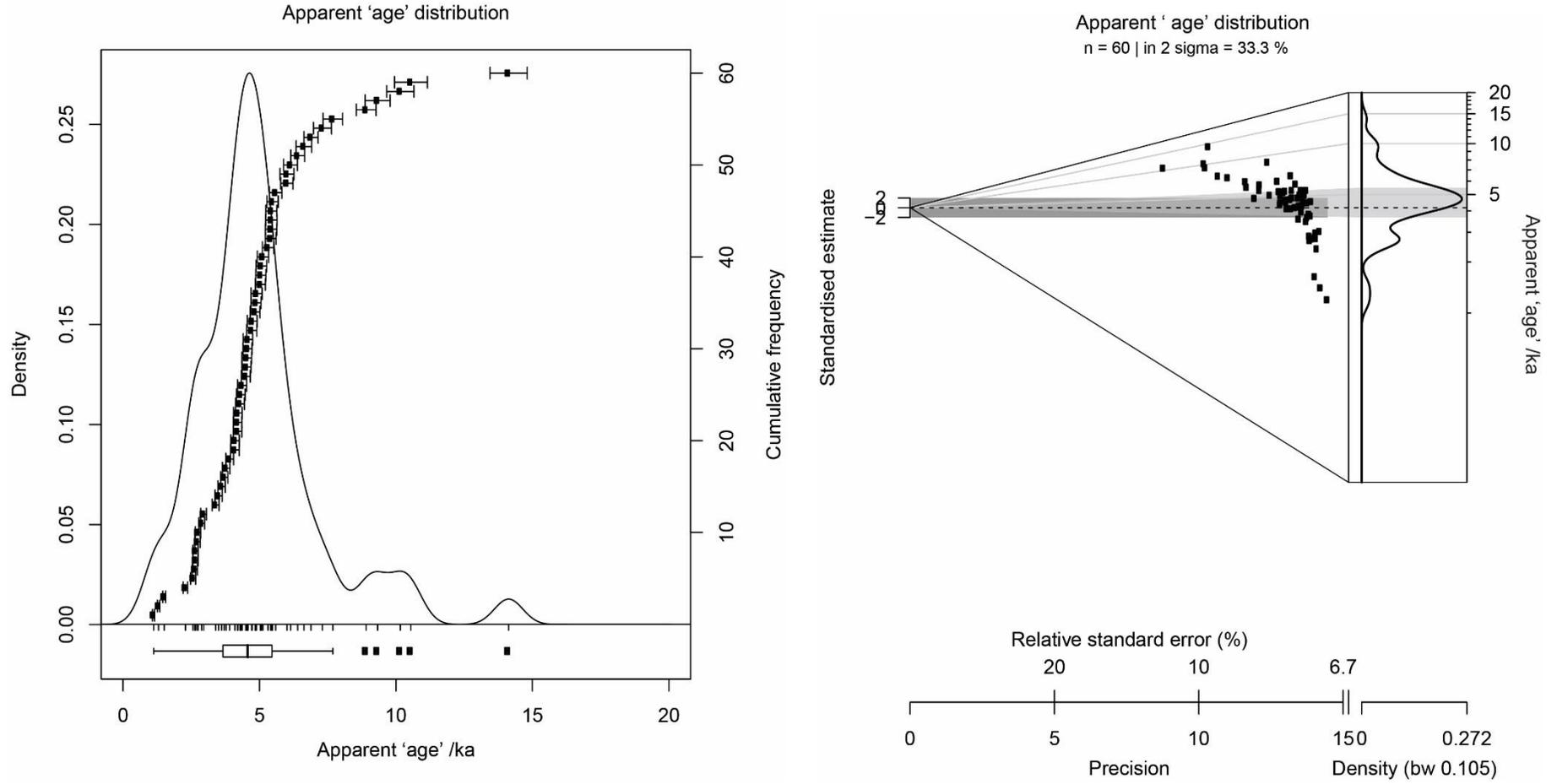
Figure A-16: Apparent 'age' distributions for CERSA237, as (left) a Kernel Density Estimate Plot, and (right) an Abanico Plot